AN ABSTRACT OF THE DISSERTATION OF

Rick L. Lawrence for the degree of Doctor of Philosophy in Forest Resources presented on January 14, 1998. Title: A Landscape-Scale Analysis of Vegetation Recovery at Mount St. Helens.

Abstract approved: Signature redacted for privacy.

William J. Ripple

I used satellite remote sensing to examine the key factors controlling the natural revegetation of Mount St. Helens since its eruption in 1980. The study required three stages: determining the amount of vegetation present; characterizing vegetation change; and analyzing the influence of factors affecting vegetation change.

To determine the amount of vegetation present, I compared various vegetation indices and multiple regression using raw spectral bands. Reference data were from interpretation of aerial photographs. A model using multiple regression on raw spectral bands provided the best results and explained 75% of the variability in vegetation cover.

To characterize vegetation change during the study period, eight Landsat Thematic Mapper satellite scenes from 1984 to 1995 were geometrically and radiometrically corrected to each other. They were then transformed to estimate green vegetation cover for each scene using the model developed in the first stage. I fit growth curves to each pixel using a combination of a non-hierarchical clustering algorithm and polynomial growth curves. To represent response variables, I extracted four parameters from the

growth curves: number of years to reach 10% vegetation cover; maximum rate of increase in vegetation cover; time-integrated vegetation cover; and maximum estimated cover reached.

Regression tree analysis explained 50%, 31%, 57%, and 51% of the variation in these response variables, respectively. Remaining variability was a function of other variables, stochastic factors and image processing. The most important determinant of revegetation was the presence or absence of biotic legacies, as evidenced by volcanic disturbance impacts. This stratified the study area into primary and secondary succession areas. Under secondary succession conditions, gradients of biotic legacies were evident. Factors affecting the establishment and growth of survivors were important, including original tephra thickness and erosional processes, evidenced by the importance of slope gradient. In primary succession areas, erosional processes were important in mitigating site conditions for colonizing seeds. Distance from seed sources was important primarily near forested edges. Additional topographic variables, including elevation, aspect, and slope curvature, had limited importance. I was not able to detect significant effects of streams, roads, or pre-eruption vegetation conditions.

A Landscape-Scale Analysis of Vegetation Recovery at Mount St. Helens

By

Rick L. Lawrence

A Dissertation Submitted

to

Oregon State University

In Partial Fulfillment of
the requirements for the
degree of

Doctor of Philosophy

Presented January 14, 1998
Commencement June 1998

Acknowledgments

I wish to acknowledge the many people and organizations who supported me throughout this endeavor.

First, and above all, to my wife, Debbie Deagen, for tolerating my continuous ramblings about esoteric problems, for proofreading and editorial reviews, for sharing me with Mount St. Helens (that demanding other woman) and, most importantly, for tireless moral and spiritual support.

To Bill Ripple, for his faith in an untried, untested, remote sensing want-to-be, and all that followed.

To Fred Swanson, for reminding me that Mount St. Helens was not just another study site, but something to be passionate about.

To all who assisted by reviewing part or all of this dissertation, including Alfredo Huete, Warren Cohen, Joseph Means, Janet Franklin, Peter Frenzen, and Jerry Franklin.

And to those who provided financial support or data to enable my research, including the National Science Foundation, the Department of Forest Resources at Oregon State University, the U.S. Forest Service Pacific Northwest Research Station, and the Washington Department of Natural Resources.

TABLE OF CONTENTS

TABLE OF CONTENTS (continued)

TABLE OF CONTENTS (continued)

LIST OF FIGURES

LIST OF TABLES

Dedication

This dissertation is dedicated to the memory of my father,

Ed Lathram.

A Landscape-Scale Analysis of Vegetation Recovery at Mount St. Helens

Chapter 1. Introduction

On May 18, 1980, Mount St. Helens in the State of Washington erupted violently, in the process creating a wealth of opportunities for scientific research. One of the primary opportunities has been the study of succession under diverse contiguous post-disturbance conditions.

Succession studies can be characterized as relating to either primary or secondary succession, although many seres, such as those following intense fires, are best classified as having characteristics of both stages (Vitousek and Walker, 1987). Most studies of succession involve secondary succession, although there have been a number of studies of primary succession, often in connection with volcanic activity. A comparison of primary and secondary succession improves our understanding of the mechanisms of succession.

The eruption of Mount St. Helens resulted in a mosaic of disturbance patterns across the adjacent landscape. The resulting landscape included a wide range of conditions, from areas devoid of life with sterile soils, to areas with propagules and organic soils under varying thicknesses of tephra but no standing vegetation, to areas of sparse surviving vegetation, to areas with no immediate loss of vegetation but with a covering of airfall tephra.

Many of the conditions created by the eruption have been studied through ground-based studies at the scale of vegetation plots or transects. While these studies have taught us much about how vegetation at Mount St. Helens is recovering, they present only part of the picture. It has been demonstrated that the structure and function of a system is scale dependent (Turner, 1989). Processes at one scale may result in patterns at another scale, and multiple scales must be examined to fully understand ecosystem processes and patterns. For successful natural resource management, disparate scales must be interfaced (Levin, 1992).

The purpose of my study was to add to our understanding of the successional processes at Mount St. Helens by examining revegetation at the landscape scale. The use of satellite remote sensing and a geographic information system makes the study of ecological patterns over a large scale feasible. Through an examination of landscape-scale patterns at Mount St. Helens, we can test our understanding of finer scale processes, thus interfacing these disparate scales. By more fully understanding the processes and patterns occurring over the variety of conditions presented by Mount St. Helens, we can achieve a better understanding of the mechanisms of succession.

My examination of succession at Mount St. Helens at the landscape scale involved three major stages, reported in the three main chapters of this dissertation. First, in order to study vegetation change, it was necessary to have a method to determine, for any one date, the amount of vegetation present. The determination of vegetation amount from remotely sensed images poses some special challenges in highly disturbed landscapes. Chapter 2 describes these challenges and presents a methodology for dealing with them.

Once vegetation amount was determined, vegetation change had to be characterized. Various characterizations are possible, depending on the question of interest. Chapter 3 describes a new, flexible method of characterizing succession using growth curves. The method relates observed changes to specific ecological responses.

Finally, once patterns of vegetation change have been characterized, they should be explained by the processes creating the patterns. Chapter 4 reports the results of my analysis of the factors affecting succession at Mount St. Helens. Specific explanatory variables were selected based on patterns and processes observed in fine-scale studies. These variables were then tested at the landscape scale to determine which variables were important in determining landscape-scale patterns.

Chapter 2. Comparisons Among Vegetation Indices and Bandwise Regression in a Highly Disturbed, Heterogeneous Landscape: Mount St. Helens, Washington

Rick L. Lawrence and William J. Ripple

Submitted to *Remote Sensing of Environment*,
University of Minnesota, St. Paul, Minnesota,
July 9, 1997, in press.

Abstract

Spectral vegetation indices have been used extensively to predict ecological variables, such as percent vegetation cover, above-ground biomass, and leaf-area index. We examined the use of various vegetation indices and multiple linear regression using raw spectral bands for predicting vegetation cover in a landscape characterized by high variability in vegetation cover and soil properties. We were able to improve the explanatory value of several vegetation indices by using regression fitting techniques including log transformations and polynomial regressions. We expected soil-adjusted indices to perform better than non-adjusted indices. However, soil-adjusted vegetation indices based on a ratio of red and near infrared bands explained 55% to 65% of the variability in vegetation cover, while two non-adjusted indices each explained 70%. An index using six spectral bands explained 40%. The best multiple regression model used the red and near infrared bands and explained 75% of the variability in vegetation cover. Among the soil-adjusted indices, an index that used a computed soil line performed best. Ratio-based vegetation indices were less sensitive to shadow influences, but this influence was out-weighed by the advantages of multiple regression against original bands.

Introduction

On May 18, 1980, Mount St. Helens in the State of Washington erupted with catastrophic, landscape-scale effects (Lipman and Mullineaux, 1981). In a mere 10 minutes, an area of approximately 500 square kilometers was devastated, with destruction of substantially all above-ground vegetation (Frenzen, 1992). The ensuing debris, mud, and pyroclastic flows further transformed the landscape from one of lush Pacific Northwest forests into a seemingly barren expanse.

The Mount St. Helens eruptions and subsequent recovery have gathered world-wide public attention. Mount St. Helens National Volcanic Monument remains one of the most visited natural wonders in the Pacific Northwest. The attention from scientists has been at least as great. A compendium published in 1994 listed 637 publications and 69 research abstracts related to the eruptions and their aftermath (Frenzen et al., 1994). However, the research opportunities afforded by Mount St. Helens have gone essentially overlooked by the remote sensing community. The research reported in this article is part of a program designed to exploit some of the remote sensing opportunities afforded by this site.

Mount St. Helens provides a nearly unique opportunity to address some of the more perplexing problems in remote sensing. Since the early days of satellite remote sensing, scientists have sought to use multispectral imagery to measure assorted ecological variables related to vegetation amount. Much of this research has attempted to formulate vegetation indices that can be related to ecological variables such as vegetation cover, biomass, leaf area index, and fraction of absorbed photosynthetically active radiation.

Considerable success has been achieved in this area. However, several problems have continued to plague remote sensing scientists. Two of these problems that are relevant to Mount St. Helens are: (1) As percentage of vegetation cover decreases, vegetation reflectance signals become increasingly contaminated by soil reflectance noise; and (2) Variation in soil reflectances increase the difficulty in adjusting for soil reflectance influences.

The area devastated by the eruption of Mount St. Helens provides the opportunity to address both of these problems in a relatively small landscape. The eruption and subsequent recovery have created substantial heterogeneity both in substrates and vegetation cover amounts. Thus, we have been able to formulate and test hypotheses related to these issues within a range of conditions that might otherwise require regional analysis.

The specific purposes of this study were twofold. First, we sought to formulate and test hypotheses regarding the relative strength of various vegetation indices that either have been widely used or were specifically designed to account for substrate influences. Second, we attempted to determine whether the use of vegetation indices to measure ecological variables has advantages over the use of multiple regression against raw, non-indexed spectral bands. We did not attempt to assess the utility of vegetation indices for other purposes, such as data visualization and data compression.

Overview of Vegetation Indices and Formulation of Hypotheses

The distinctive spectral properties of green vegetation have long been used by remote sensing scientists to map ecological variables of interest. Jordan (1969) is credited with first combining near infrared and red spectral responses into a ratio that was then shown to correlate highly with leaf-area index. Since that pioneering work, a vast number of spectral band combinations have been studied as measures of vegetation. These vegetation indices have been variously proposed, modified, analyzed theoretically, compared, summarized, categorized, and criticized. Although it is not our intent to repeat those efforts here, we will review certain vegetation indices to the extent necessary to formulate hypotheses regarding which indices should perform relatively better under the heterogeneous vegetation and substrate conditions found within the Mount St. Helens devastated area.

We have generally divided vegetation indices into two categories, although other categorizations might be appropriate for other purposes. The first types are ratio-based indices. The most commonly used of these indices exploit the characteristic chlorophyll absorption by vegetation in the red portion of the spectrum and high reflectance by vegetation in the near infrared portion (Tucker, 1979). Ratio-based indices include the simple ratio (SR) developed by Jordan (1969), the normalized difference vegetation index (NDVI) developed by Rouse et al. (1973), and various modified versions of NDVI designed to address its sensitivity to factors such as soil variability and atmospheric conditions. The formula for each vegetation index discussed in this paper is presented in Table 1.

Table 1. Formulae for vegetation indices used in this paper. Band designations are for Landsat TM bands -- band 1 = 0.45-0.52 µm, band 2 = 0.52-0.60 µm, band 3 = 0.63-0.69 µm, band 4 = 0.76-0.90 µm, band 5 = 1.55-1.75 µm, band 7 = 2.08-2.35 µm. Band 6, used in the bandwise regression analysis, is 10.4-12.5 µm.

Index	Formula
SR	$SR = \frac{Band4}{Band3}$
NDVI	$NDVI = \frac{Band4 - Band3}{Band4 + Band3}$
SAVI	$SAVI = \frac{1.5 * (Band4 - Band3)}{Band4 + Band3 + 0.5}$
OSAVI	$OSAVI = \frac{1.16 * (Band4 - Band3)}{Band4 + Band3 + 0.16}$
TSAVI	$TSAVI = \frac{a * (Band4 - (a * Band3) - b)}{Band3 + (a * (Band4 - b)) + (0.08 * (1 + a^2))}$ where: a = the slope of the soil line b = the intercept of the soil line
$MSAVI_2$	$MSAVI_2 = \frac{(2 * Band4) + 1 - ((2*Band4) + 1)^2 - (8 * (Band4 - Band3))^{0.5}}{2}$
GVI	GVI = -(0.2848 * Band1) - (0.2435 * Band2) - (0.5436 * Band3) + (0.7243 * Band4) + (0.0840 * Band5) - (0.1800 * Band7)

A second type of indices are soil-line based or orthogonal indices. These indices are based on there being a line in spectral space (assuming two dimensions, a plane in three dimensions, or a hyper-plane in higher dimensions) along which bare soils of differing brightness will lie. Vegetation increases perpendicularly to the soil line. Kauth and Thomas (1976) developed their "tasseled cap" transformation for Landsat MSS data, the second component of which has become known as the greenness index, which is sometimes called the green vegetation index (GVI). Crist and Cicone (1984) have extended the analysis to six bands of Landsat Thematic Mapper (TM) data (excluding the thermal infrared band). We used the version of this index currently implemented in the Imagine 8.2 image processing software (ERDAS, 1995).

The reader is referred to the original works cited above for more detail on the theory and derivation of these vegetation indices, as well as several excellent reviews contained in the literature (e.g., Rondeaux et al., 1996; Qi et al., 1994; Perry and Latenschlager, 1984). Specific properties of the indices relevant to our study will be discussed below in connection with hypothesis development.

Ratio-based Indices

The two most widely used ratio-based indices are SR and NDVI. These indices have performed well in many applications, showing high correlations to vegetation cover, above-ground biomass (Tucker, 1979; Elvidge and Lyon, 1985; Anderson et al., 1993), leaf-area index (Running et al., 1986; Spanner et al., 1990), and other ecological variables (e.g., Cihlar et al., 1991; Myneni and Williams, 1994; Yoder and Waring, 1994; Wiegand et al., 1991). Coefficients of determination (R^2s) between these variables and ratio-based indices ranging from 0.60 to 0.90 have been reported in many studies (although some studies have had lesser or greater degrees of success). Based on a rational theory for the correlation of SR and NDVI to green vegetation cover, as well as the empirical success of other studies, we formulated a baseline hypothesis:

Hypothesis 1: Vegetation cover within the Mount St. Helens devastated area is significantly correlated to SR and NDVI.

We called this our baseline hypothesis because it referred to the simplest of the vegetation indices, and we formed our further hypotheses relative to Hypothesis 1.

Notwithstanding the observed success of SR and NDVI, these indices were found to have limitations because of their sensitivity to different substrates (Huete, 1988).

Several modified versions of NDVI have been developed, with increasing complexity, to reduce the inherent sensitivity of NDVI to varying substrates. The soil-adjusted vegetation index (SAVI) (Huete, 1988) incorporates an adjustment factor, based on the amount of vegetation, from 0 (for high vegetation) to 1 (for low vegetation). In the absence of extrinsic knowledge, an intermediate adjustment factor of 0.5 has been suggested and generally applied. Our study area is highly variable with respect to vegetation amount, with substantial areas low in vegetation. Therefore, if the rationale behind SAVI is sound, it should perform better than NDVI for Mount St. Helens.

A minor, but potentially important, variation to SAVI has been proposed by Rondeaux et al. (1996). An approach to optimizing the adjustment factor for general applications resulted in a recommended adjustment factor of 0.16, rather than 0.5. The optimized soil-adjusted vegetation index (OSAVI) is the same as SAVI with an adjustment factor of 0.16. Once again, if the rationale behind OSAVI is accepted, we expect OSAVI to out perform SAVI throughout the range of vegetation covers present at Mount St. Helens. However, because of the relatively low average vegetation within the study area, we hypothesized that the higher adjustment factor of SAVI might result in better performance at Mount St. Helens than OSAVI.

Rather than using a universal adjustment factor, the transformed soil-adjusted vegetation index (TSAVI) uses the slope and intercept of the specific soil line of the study area (Baret et al., 1989). Although the adjustment to NDVI is based on the soil line, rather than vegetation amount, the effect is similar in moving the assumed location of the soil line and how vegetation varies from the soil line. TSAVI specifically adjusts to a given study area. As a result, we can expect it to perform better than the "universally" adjusted SAVI and OSAVI. However, we also note that TSAVI assumes that there is a well defined soil line. With the substrate variability present at Mount St. Helens, this may not be true.

The final ratio-based index we examined was the modified soil-adjusted vegetation index (MSAVI) (Qi et al., 1994). MSAVI is designed to correct a weakness in SAVI in how vegetation responds as it moves away from the soil line. MSAVI has the same conceptual basis as SAVI. However, with MSAVI vegetation isolines (lines of equal vegetation) cross the soil line at varying points. This is believed to more accurately reflect how vegetation spectral responses actually behave. Because of this improvement over SAVI, we expect MSAVI to perform better than SAVI, OSAVI, or TSAVI. (For this study, we used the second of the proposed versions, $MSAVI_2$, which does not require an empirically determined soil line.)

Based on the theory presented for each soil-adjusted index and the results observed by the developers of these indices, we can present a second, multi-part hypothesis.

Hypothesis 2: For the Mount St. Helens devastated area, soil-adjusted vegetation indices (a) are highly correlated to vegetation cover, (b) explain more variation in vegetation cover than non-adjusted indices, and (c) perform in increasing ability in the order OSAVI, SAVI, TSAVI, and $MSAVI_2$.

Orthogonal Indices

Widely used orthogonal vegetation indices are based on a universally pre-determined soil line, rather than the inherently assumed soil line underlying NDVI. Therefore, orthogonal indices have not been subject to modifications similar to the soil-adjusted versions of NDVI. The most widely used orthogonal index is the tasseled cap greenness index, or green vegetation index (GVI). By using six bands, rather than the two used in ratio-based indices, the Landsat Thematic Mapper version of GVI has the potential for making greater spectral distinctions in vegetation. In certain cases, perpendicular indices have been found superior in correlations to vegetation variables than ratio-based indices (Huete and Jackson, 1988). However, much of the variability in vegetation versus soil occurs in the red and near infrared portions of the spectrum, while variation in soil types is often detected in middle infrared bands (Lillesand and Kiefer, 1994). Thus, we postulated that, under conditions of low vegetation cover and substrate heterogeneity, GVI might be more sensitive to soils than ratio-based indices, resulting in reduced ability to distinguish differences in vegetation cover. This leads us to our third hypothesis.

Hypothesis 3: GVI will explain less variability in vegetation cover within the Mount St. Helens devastated area than ratio-based indices.

Multiple Regression Approach

Vegetation indices have been advocated for vegetation analysis because they provide a standardized approach to analysis. Although this argument has some appeal, we question its validity when there is a need to estimate or predict ecological variables (as opposed to using indices for data visualization purposes, for example). Rather, if the study requires knowledge of an ecological variable of interest (e.g., above-ground biomass), the researcher must ultimately analyze the relationship between the spectral index used and the ecological variable, generally through a regression analysis. For example, several studies have found high correlations between NDVI and leaf-area index (LAI) (e.g., Running et al., 1986; Spanner et al., 1990; Chen and Cihlar, 1996). However, the nature of the relationship varies with each study so that we cannot say that a certain NDVI generally equals a certain LAI. For example, when we used the two regression formulae published by Spanner et al. (1990) for two different years, and assumed an NDVI value of 0.5, the estimated LAI differed by 5.5% between the two scenes. Chen and Cihlar (1996) showed that the regression formula can differ between seasons.

The use of vegetation indices would seem to unnecessarily constrain the regression analysis. For example, many studies using NDVI or SR fit both a simple linear model (of the form $y = \beta_0 + \beta_1 x$ where y = an ecological variable of interest and x = a spectral vegetation index) and test for a curvilinear relationship by using a log-transformed response variable (presented either as $\log(y) = \beta_0 + \beta_1 x$ or $y = \beta_0 e^{\beta x}$). However, these models using vegetation indices are not able to independently model the red and near infrared responses. Thus, if the red response is curvilinear and the near infrared is not, a compromise fit is necessary. Further, regression model fitting using band interactions, polynomial terms, and other data transformations are similarly constrained because any function performed on the index affects both bands proportionately and simultaneously. At least one study has found regression on individual bands to explain more variability than regression against NDVI (Ripple, 1994), although the causes of this effect have not been explored. This leads us to our fourth, and final, hypothesis.

Hypothesis 4: Multiple linear regression on individual bands will explain as much or more of the variability in vegetation cover within the Mount St. Helens devastated area than any vegetation index.

Study Area

The 1980 eruptions of Mount St. Helens may be the most heavily documented volcanic eruptions in history. In one sense, the May 18 eruption may be viewed as a single catastrophic event. However, for most ecological purposes it is best viewed as a related suite of disturbance events that resulted in a complex mosaic of disturbed patches. Although minute-by-minute accounts of the events have been presented (e.g., Lipman and Mullineaux, 1981), one paragraph by Franklin et al. (1985:201) provides a thumb-nail sketch:

> The 18 May 1980 eruption began at 0832 PDT when a large earthquake triggered a massive avalanche of debris involving the entire upper portion of the mountain. Movement of this mass unroofed the core of the mountain where superheated groundwater flashed to steam, unleashing a blast of steam and rock debris in a 180° arc to the north. Mudflows rampaged through the valley-bottom forests to the west and southeast. Volcanic ash rained from the sky to the northeast of the mountain from the morning of 18 May into the next day. In early afternoon of 18 May and during the subsequent eruptions, pumiceous pyroclastic flows (flows of hot gases and pumice) spilled northward out of the newly formed crater across the deposits left by the avalanche.

The effects were clearly devastating throughout the affected area. Disturbed areas were generally well defined depending on the type of disturbance affecting them. Thus, the resulting landscape is a mosaic of deposits from the debris avalanche, pyroclastic flows, mudflows, downed timber, scorched vegetation, and airfall tephra. Each of these deposits has distinctive characteristics regarding thickness, deposit temperature, and substrate composition (Franklin et al., 1988). As a result, potential spectral properties of the substrate and potential rates of vegetative recovery vary significantly throughout the area.

The specific selection of our study area was dictated by the larger study of which this research is a part. That larger study is examining the natural recovery of the area devastated by the 1980 eruptions. Therefore the study area was limited to that portion of the devastated area that has not been reforested following the eruption. Large water bodies within the area were also excluded. Figure 1 is a false color composite of the study area using the TM image acquired for this study. The study area consisted of approximately 25,400 hectares, or approximately 42% of the area devastated by the eruption.

Figure 1. False color composite of study area from Landsat TM image. Band 4 (near infrared) is displayed in red, band 3 (red) is displayed in green, and band 2 (green) is displayed in blue.

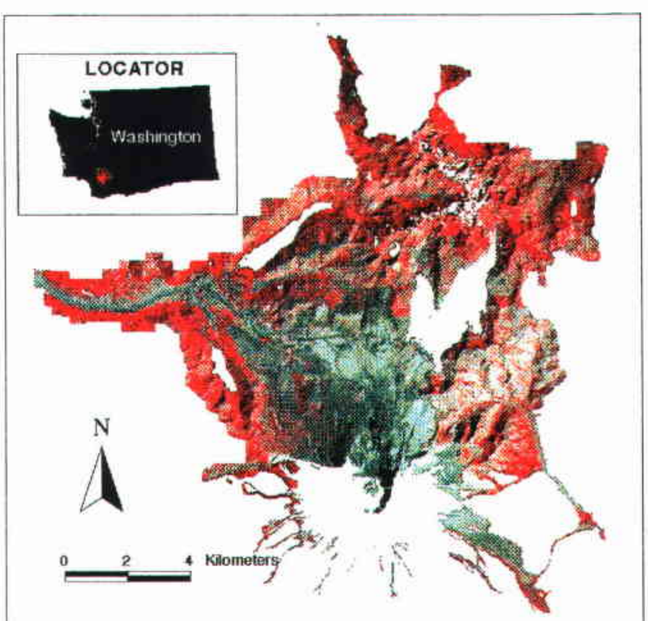

Vegetation structure and types are not readily summarized for the study area because plant cover is highly variable, within site plant diversity is often high, and successional changes are, in some cases, rapid, making previous reports rapidly obsolete. Early reports of vegetation in blowndown forests reported 0.2% mean canopy cover in 1981, with dominant species primarily herbaceous, including pearly everlasting (*Anaphalis margaritacea)*, thistle (*Cirsium* spp.), fireweed and willowweeds (*Epilobium* spp.), ryegrass (*Lolium* spp.), and groundsel (*Senecio* spp.) (Franklin, et al., 1985). By 1992, these species had completely covered portions of the landscape (Frenzen, 1992). In subalpine study sites, substantially different results have been reported (del Moral and Bliss, 1993). Recovery has varied depending on the nature of the disturbance, with less than 1% cover reported on pyroclastic flows, under 5% on mudflows, and over 40% on adjacent tephra covered sites. Although there is significant overlap in species composition among these sites, dominance varies greatly. Most abundant species in order of importance in 1990 included on tephra sites bentgrass (*Agrostis diegoensis),* prairie lupine (*Lupinus lepidus*), spreading phlox (*Phlox diffusa*), and Newberry fleeceflower (*Polygonum newberryi*), and on a mudflow Newberry fleeceflower, prairie lupine, and Cardwell's penstemon (*Penstemon cardwellii*). However, there was significant change in the relative importance of species on the mudflow site between 1988 and 1990, emphasizing the rapid changes taking place within the area. Although tree species are not yet of significant influence within the Mount St. Helens devastated area, in some areas late snowpacks at the time of the eruption protected mountain hemlock (*Tsuga mertensiana*) and Pacific silver fir (*Abies amabilis*), scattered alder (*Alnus* spp.) and Douglas-fir (*Pseudotsuga menziesii*) have appeared throughout the area, and some roots of willows

(*Salix* spp.) and black cottonwood (*Populus trichocarpa*) that were up-rooted by mudflows and the debris avalanche happened to come to rest at the surface and resprout (Frenzen, 1992).

Methods

Data Acquisition

The study area was extracted from a 19 August 1995 TM scene (path 46, row 28). We received the data rectified to a Universal Transverse Mercator (UTM) grid using a cubic convolution resampling method.

The study area was subset using a mask created from four GIS layers. The Gifford Pinchot National Forest (GPNF) provided a layer defining the boundaries of the Mount St. Helens National Volcanic Monument (the Monument). Areas outside the Monument were subject to reforestation and were masked from the study area. A stand data layer provided by GPNF was used to exclude the few stands within the Monument that were reforested. A disturbance map prepared by the USGS (Lipman and Mullineaux, 1981) was manually digitized and used to delineate those areas within the Monument that were devastated by the eruptions. Finally, an unsupervised classification of the study area portion of our Landsat scene, using the ISODATA algorithm (ERDAS, 1995), was used to identify large water bodies and exclude them from the study area. The resulting study area image is shown in Figure 1.

Reference data were provided by interpretation of true color aerial photographs (1:15,840) loaned to us by the Monument. The aerial photographs were acquired in late June through late July, 1995. Ground visits to the study area were conducted with copies of aerial photographs during summer 1996. During these visits, we delineated examples of different cover conditions on the aerial photographs as an aid to aerial photo interpretation.

Sampling Procedure

Prior to sampling the data, we determined the number of samples necessary to detect differences in vegetation indices of significance. We intended to estimate vegetation cover from the aerial photos in increments of 10%. Therefore, we needed sufficient samples to detect, with 95% confidence, half width differences of this increment, or 5%. Using the procedures outlined in Montgomery (1991), we determined that 95 sample points would be adequate for all of the vegetation indices we examined. This sample size was confirmed by applying the same procedures to our estimates of vegetation cover after our aerial photo interpretation was completed. We acquired 200 sample points to account for the possibility of having to screen out some points and potential curvilinear relationships between indices or raw TM bands and vegetation cover.

A random set of sample points was generated for the Landsat image using Imagine 8.2 image processing software's accuracy assessment program (ERDAS, 1995). Actual sample plots included a three-pixel-by-three-pixel area with the sample point at its center. We selected this plot size because we were confident we could accurately locate plots of this size on the 1:15,840 scale aerial photos. We eliminated 32 points for the following reasons: (1) 17 points because they were affected by snow cover, generally within the volcano's crater; (2) eight points because they were too close to the edge of the study area to obtain a three-by-three pixel plot; (3) five points because the aerial photograph was missing; (4) one point because the plot was partially covered by a pond; and (5) one point because it duplicated another point. The final set of 168 points was used for all statistical analysis reported in this paper.

For each sample plot we recorded the average digital number (DN) values for each TM spectral band. SR, NDVI, and GVI were computed from these DN values. For the soil-adjusted indices, DN values were transformed to exoatmospheric reflectance units prior to computing index values (Markham and Barker, 1986).

Each sample plot was located on the aerial photos using landmarks identifiable on both the photos and the Landsat image. Plots were marked, labeled, and interpreted. For each plot, we made visual estimates of the percentage of the plot covered by (1) green vegetation and (2) shadow. All estimates were made in 10% increments because we felt this was the reasonable limit of differentiation possible with visual interpretation. Thus, estimates of 1% to 10% cover were classified as 5%, 11% to 20% as 15%, and so on. In addition, estimates of 0% cover were recorded.

Statistical Analysis

Prior to performing any regression analysis, and to assist in the selection of regression models, we examined exploratory graphs of the data. Boxplots (Figure 2) of NDVI, soil-adjusted indices and GVI showed no significant departures from symmetry. Both SR and percentage of green vegetation cover (Veg Cover) as interpreted from the aerial photos showed some degree of skewing, indicating the potential advantages of data transformation, such as a log transformation. Plots of Veg Cover versus individual bands and indices revealed no unexpected trends, other than some possible curvilinear relationships.

Figure 2. Boxplots for vegetation indices used in this study and percent of green vegetation cover as interpreted from aerial photographs. Plots do not show substantial deviations from symmetry, except for SR and percent of vegetation cover, which are skewed toward lower values, indicating possible advantages of data transformations.

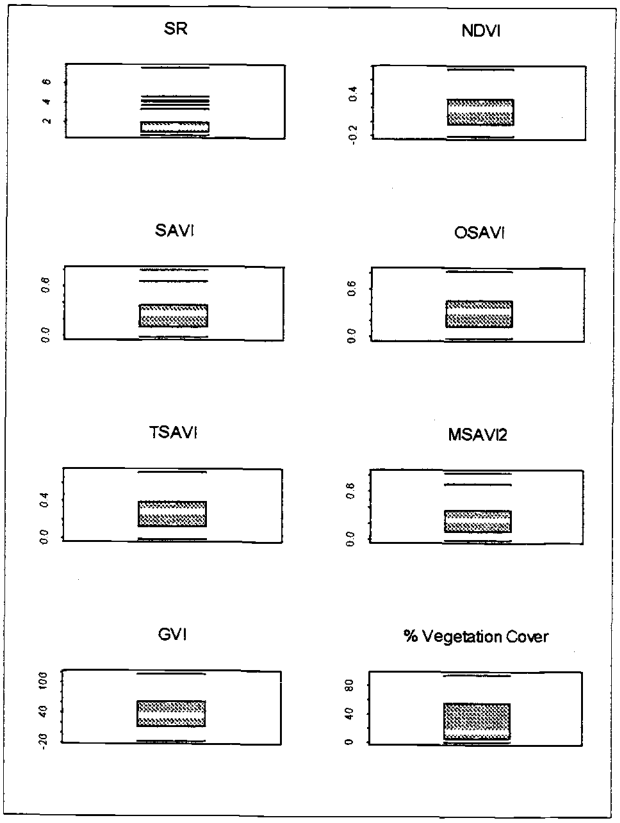

Simple linear regression was used to initiate analyses of individual vegetation indices. For each index, analysis of residual plots and exploratory data plots was used to guide potential improvements in the regression fits. Extra-sum-of-squares F-tests were used to evaluate the significance of additional predictor variables, and coefficients of determination (R^2) were examined to determine the amount of variability explained by the best fitting models. To avoid infinite values, for log transformations of variables containing 0 values, a value was added to the variable equal to 0.01 times the smallest incremental value of the variable. (For example, for vegetation cover, which was recorded in integer increments, a value of 0.01 was added to each entry, so that for a sample plot with no vegetation, we used a value of log 0.01.)

Forward and backward stepwise regression was used with all seven TM bands to provide guidance as to which bands might be significant in predicting Veg Cover. As with vegetation indices, residual and exploratory data plots were used to guide further regression analysis and select the best fit.

Results

Vegetation Indices

Regression models for the vegetation indices using simple linear regression and models with a log-transformed response variable (log-transformed models), as has been traditionally used in vegetation index studies (e.g., Anderson et al., 1993; Chen and Cihlar, 1996; Friedl et al., 1995; Jordan, 1969; Spanner et al., 1990; Yoder and Waring, 1994), were all statistically highly significant (p-values < 0.0001). Table 2 sets forth R^2s for each

Table 2. Results of linear and log-transformed regressions of percentage of vegetation cover against vegetation indices. Log transformations did not improve any regressions, except for GVI. NDVI explained the most variation (65%) and GVI explained the least (40%).

Index	Linear Regression R^2	Log-Transformed Regression R^2
SR	0.6002	0.3502
NDVI	0.6539	0.5900
SAVI	0.5515	0.5001
OSAVI	0.5912	0.5535
TSAVI	0.6184	0.5796
$MSAVI_2$	0.5546	0.4782
GVI	0.3261	0.4025

of these models. NDVI performed best (best $R^2 = 0.65$), followed by TSAVI (best $R^2 = 0.62$), SR (best $R^2 = 0.60$), OSAVI (best $R^2 = 0.59$), $MSAVI_2$ (best $R^2 = 0.55$), and SAVI (best $R^2 = 0.55$). GVI performed substantially worse (best $R^2 = 0.40$).

We found that we could improve on several of these models by including polynomial terms in the final regression models. Other transformations, including additional log, inverse, and square-root transformations, did not significantly improve

Table 3. Final regression models for percentage of vegetation cover estimated from aerial photos against individual vegetation indices. Variables were tested for significance using extra-sum-of-squares F-tests. Ratio-based indices that have not been soil adjusted (SR and NDVI) explained the most variation (70%), followed by soil-adjusted indices (55% to 65%). GVI explained substantially less variation (40%).

Index	Regression Model	Multiple R^2
SR	Veg Cover = 29.53 + 312.63 (log SR) + 33.18 $(\log SR)^2$ - 64.12 $(\log SR)^3$	0.6982
NDVI	Veg Cover = 9.78 + 45.35 NDVI + 105.11 $NDVI^2$ + 510.84 $NDVI^3$ - 725.10 $NDVI^4$	0.7040
SAVI	Veg Cover = -1.91 + 143.77 SAVI	0.5515
OSAVI	Veg Cover = 3.86 - 20.50 OSAVI + 436.40 $OSAVI^2$ - 327.86 $OSAVI^3$	0.6166
TSAVI	Veg Cover = 3.34 - 33.74 TSAVI + 540.63 $TSAVI^2$ - 423.81 $TSAVI^3$	0.6476
$MSAVI_2$	Veg Cover = -0.68 + 124.65 $MSAVI_2$	0.5546
GVI	log(Veg Cover) = -0.73 + 0.066 log(GVI)	0.4025

model results. Table 3 sets forth for Veg Cover regressed against each vegetation index the final regression model selected and the multiple R^2 representing the amount of variation explained by the model. Although some of the final models selected may be more complex than may be desirable for the additional amount of variation explained over the simple models, only by fitting the best regression model can the indices be objectively compared. Choosing a simpler model involves subjective judgments as to what level of model complexity is worthwhile and compromises an objective comparison. The extra-sum-of-squares F-test is a rigorous standard for the addition of predictor variables and only allows the addition of variables that are significant when considered with other variables already in the model.

All final regression models were statistically highly significant (all p-values < 0.0001). R^2s for the final regression models for the ratio-based vegetation indices ranged from 0.55 to 0.70. Final models for SAVI and $MSAVI_2$ were simple linear regressions. OSAVI and TSAVI included third degree polynomials, while NDVI included a fourth degree polynomial. SR was the most complex model and included a log transformation of SR and a third degree polynomial.

The final regression model for GVI explained substantially less variation than the ratio-based indices, with an R^2 of 0.40. This model included a log-log transformation and no polynomial terms.

Bandwise Regression Models

Simple linear and log-transformed regressions of individual bands against Veg Cover were performed to determine the basic relationships between our variable of interest and the bands. Table 4 sets forth the slopes, p-values, and R^2s for these regressions. Veg Cover varied inversely with all bands except bands 4 (near infrared) and 5 (middle infrared). Each band individually in a simple regression was able to explain at least one-fourth of the variation in Veg Cover, except band 6 (thermal infrared), which explained 18% of the variability, and bands 5 and 7 (middle infrared), which explained 2%

Table 4. Results of linear and log-transformed regressions of percentage of vegetation cover against individual spectral bands. Signs of slope terms indicate positive correlations with bands 4 and 5 and negative correlations with all other bands. Linear relations provide better fits with all bands except band 5.

TM Band	Linear Regression			Log-Transformed Regression		
	Slope	p-value	R^2	Slope	p-value	R^2
Band 1	-1.69	<0.0001	0.4281	-0.17	<0.0001	0.3605
Band 2	-2.64	<0.0001	0.3343	-0.25	<0.0001	0.2495
Band 3	-1.80	<0.0001	0.4363	-0.16	<0.0001	0.3070
Band 4	0.75	<0.0001	0.2729	0.079	<0.0001	0.2517
Band 5	0.19	0.06843	0.01974	0.050	<0.0001	0.1118
Band 6	-1.81	<0.0001	0.1769	-0.16	<0.0001	0.1120
Band 7	-0.70	0.001375	0.05964	-0.019	0.4342	0.003667

and 6% of the variability, respectively. Only band 5 performed better in a log-transformed model, with 11% of variability explained.

Forward stepwise regression on all seven TM spectral bands against non-transformed Veg Cover resulted in a model including bands 3 (red), 4 (near infrared), and 6 (thermal infrared). All three bands were highly significant (all p-values < 0.01), the model was highly significant (p-value < 0.0001), and the multiple R^2 was 0.69. However, a review of the residual plots from the regression showed potential curvature in the fit. Review of residual plots, exploratory data plots, and stepwise regression including polynomial terms was used to guide further model fitting. The final fitted bandwise regression model was:

$$\textbf{Veg Cover} = \mathbf{106.00 - 5.50\ (band\ 3) + 0.048\ (band\ 3)^2 + 1.36\ (band\ 4) - 0.0051\ (band\ 4)^2}$$

The regression model and each model term were highly significant (all p-values < 0.0001), except for the (band 4)^2 term, which was significant (p-value = 0.0135), and the multiple R^2 was 0.75.

Effect of Shadows

We regressed each vegetation index and the final bandwise regression model against the percent of shadow cover in each plot from our aerial photo interpretation to determine the relative sensitivity to shadow influence. Most shadows were the result of topography and standing dead trees. Live vegetation was rarely tall enough to cause substantial shadowing. Shadow was not significant for any of the ratio-based indices (all p-values > 0.5). However, percent of shadow was marginally significant for GVI (p-value = 0.13) and highly significant for the bandwise model (p-value = 0.003). Of our 168 plots, 44 had at least 5% shadow coverage.

Discussion

Ratio-Based Indices -- Hypotheses 1 and 2

As predicted in Hypotheses 1 and 2(a), all ratio-based indices were significantly correlated to vegetation cover. This result was expected based on the known biophysical relationships between red and near infrared reflectance and green vegetation. Further, the variation explained by the best of these individual indices was substantial (65% to 70%) and well within the range found by previous studies. We expected several sources of unexplained variation would prevent higher R^2 values, including (1) the estimation of vegetation cover in 10% increments incorporated variation within these ranges, (2) phenologic changes in vegetation during the one to two months between aerial photo and satellite image acquisition were not accounted for, and (3) vegetation cover amounts with differing leaf-area indices were treated as equal, although it is known that higher leaf-area indices can affect spectral responses.

This last source of variability illustrates an important limitation on the accuracy of vegetation indices. For example, two plots might each have 50% vegetation cover. Within the portion of the plot covered by vegetation, one plot might have an LAI of 2 while the other has an LAI of 4. Because the deeper canopy reflects more near infrared and absorbs more red, the second plot will have a higher vegetation index, all other factors being equal. We expect this variability might be especially noticeable at high cover amounts, where LAI can continue to increase while increases in percent cover are limited.

All ratio-based indices except SAVI and $MSAVI_2$ incorporated polynomial terms in their best regression fits. It has been found in previous studies that vegetation indices often have a curvilinear fit to LAI because the spectral response saturates beyond a certain point (Ripple, 1985). We believe that the effect of varying leaf areas also results in curvature in our study. We hypothesize that, as vegetation cover increases, leaf area within patches of vegetation also tends to increase. For example, as vegetation initially invades a barren site, most patches are made up of annuals or juvenile plants. Further occupation of the site may include new invaders, but will also result from the expansion and aging of plants already present. This in turn leads to deeper canopies and, especially in the red band, greater absorption for the amount of vegetation cover. For example, percent vegetation cover might increase within a sample plot from 20% to 40%, while in-patch LAI increases from 2 to 4. In this case, the sample plot LAI increases from 0.4 to

1.6, a four times increase in LAI with a two times increase in percent vegetation cover. The response is, therefore, curvilinear.

The simple linear, log-transformed, and final models do not support Hypothesis 2(b), but do partially support Hypothesis 2(c). Both SR and NDVI explained more variability than any of the soil adjusted indices. TSAVI did better than SAVI and OSAVI, as hypothesized, but $MSAVI_2$ did not. Finally, OSAVI performed better than SAVI, contrary to expectations.

We believe that our results are explained by the particular soil line present in our study. We estimated the soil line for the soil-adjusted indices to have an intercept of -0.02 and a slope of 1.1. Reflectance values used in calculating these indices range from 0 to 1. Thus, the intercept and slope are not substantially different from 0 and 1, respectively. These soil line parameters are the same as inherently assumed for NDVI and SR and might explain the superior performance of these indices. TSAVI uses the computed soil line parameters and, probably for this reason, performed better than other soil-adjusted indices. OSAVI uses a smaller correction (0.16) than our implementation of SAVI (0.50), and thus diverged less from NDVI. We believe that MSAVI might have performed better if we had used $MSAVI_1$, which uses computed soil line parameters.

Although for our study area SR and NDVI explained more variation than soil-adjusted indices, our analysis indicates that the basis underlying soil-adjusted indices is sound. Adjustment of indices in accordance with soil line parameters improved results. In our case, these parameters were not substantially different than those assumed in unadjusted indices. However, these results also point to the importance of using actual soil line parameters. When "universally" applicable parameters were applied, as in SAVI and OSAVI, results were inferior to unadjusted indices.

GVI -- Hypothesis 3

GVI was significantly correlated to vegetation cover but, as predicted by Hypothesis 3, explained substantially less variation than ratio-based indices. The relatively poor response of GVI might be explained by the relatively low vegetation cover (and consequent high substrate exposure) in the study area, combined with the inclusion of middle infrared bands in the calculation of GVI. The middle infrared portion of the spectrum is known to be sensitive to soil mineral content. Our study area is characterized by a heterogeneous mosaic of soils poor in organic matter. The reflectances of these soils can be expected to be heavily influenced by mineral content and other substrate characteristics, which vary throughout the area (Hoblitt et al., 1981; Ugolini et al., 1991). The influence of this soil variation on the middle infrared bands probably added significant noise to the predictor variable, thereby interfering with the relationship that we observed with the red and near infrared bands.

Table 5. Coefficients of variation for each Landsat TM spectral band for bare soil sample plots indicate the relative amount of variability in soil reflectance for each band. The middle infrared bands 5 and 7 show substantially more variability than other bands.

Band	Coefficient of Variation
Band 1	0.12
Band 2	0.17
Band 3	0.22
Band 4	0.09
Band 5	0.36
Band 6	0.03
Band 7	0.31

To confirm the effects of soil on different bands, we calculated the coefficients of variation for each band for all sample plots with no vegetation cover. The results are presented in Table 5. The coefficient of variation normalizes the variability for each band and reflects the relative amount of variability in bare soil for each band. Bands 5 and 7 show substantially more variability in soil response than other bands. Therefore, the inclusion of these bands in an index increases the amount of information contained in the index that is not related to vegetation cover.

Bandwise Regression -- Hypothesis 4

The results of our regression against the raw, non-indexed bands supports our hypothesis that this approach has the potential for out performing vegetation indices. The regression model was highly significant and explained between 5% and 20% more variation than the ratio-based vegetation indices. Figure 3 displays the estimated percentage of vegetation cover for the study area based on the final bandwise regression model. An examination of the bandwise regression model explains why this approach can be superior to vegetation indices.

Figure 3. Estimated vegetation cover for the study area based on the application of the final bandwise regression model: Percent vegetation cover = 106.00 - 5.50 (band 3) + 0.048 (band 3)^2 + 1.36 (band 4) - 0.0051 (band 4)^2. p-value < 0.0001. Multiple R^2 = 0.75.

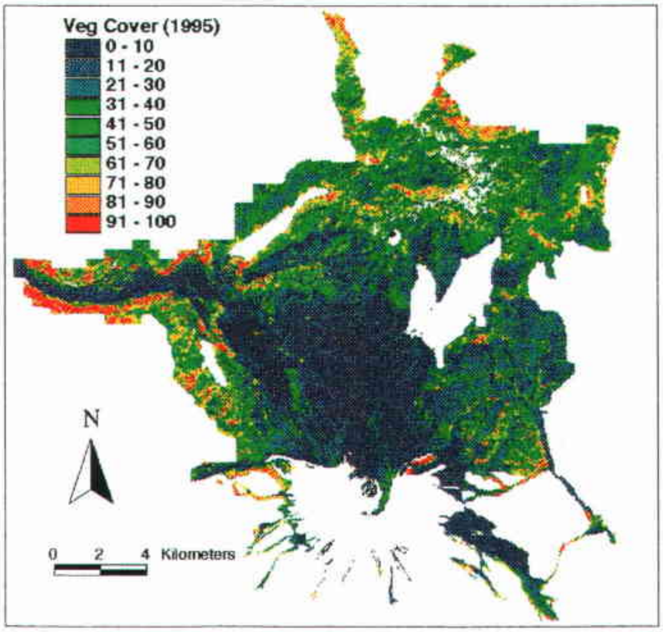

The final bandwise regression model includes only bands 3 and 4, as do the ratio-based vegetation indices. Thus, like the vegetation indices, the bandwise model is a function of these two bands. Further, as with several of the ratio-based models, the bandwise model includes a term reflecting a curvilinear relationship (the squared red and near infrared bands). However, the relative influence of the bands and their polynomials is markedly different. For example, the red band has over four times the influence of the near infrared band, and the squared infrared band has about one-tenth the influence of the squared red band. This might be the result of the red band having a much lower spectral asymptote than the near infrared band (Ripple, 1985). Thus, the bandwise regression approach allows the decoupling of bands and permits the analyst to discover different relationships between the response variable and each band, including different polynomials, coefficients, and transformations. This flexibility is not possible with regression against vegetation indices. Further, because different biophysical mechanisms control different band responses, there is no reason to believe the relation of individual bands to ecological variables will necessarily be the same.

Using bandwise regression did not require substantial additional time when compared to the use of vegetation indices. With both approaches, we had to perform regression analysis to relate spectral responses to our ecological variable of interest. The only additional step required for the bandwise regression was the selection of spectral bands as predictor variables. This step should take a few hours, at most, which we believe is not a significant increase in time for most projects. Further, this additional step can be eliminated if only the red and near infrared bands are employed. Although the exclusive use of these two bands is not unreasonable, considering our results and those of previous studies, we believe that testing other spectral bands is prudent. The success in other study areas of multiband orthogonal indices, as well as indices using middle infrared (e.g., Dusek et al., 1985) and thermal infrared bands (Boyd and Ripple, 1997), indicates that the optimal selection of spectral bands might depend on the individual scene and parameter being estimated.

Models that were not ratio-based (GVI and the bandwise model) were more sensitive to shadows than ratio-based indices. However, in spite of a large percentage of our plots with shadow influence, the bandwise model performed better than the ratio-based indices. Thus, any reduced sensitivity of ratio-based indices to shadows appears to be out-weighed by the other advantages of bandwise multiple regression.

Summary and Conclusion

Under conditions of high substrate and vegetation heterogeneity, all vegetation indices were found to be highly correlated to green vegetation cover. Among ratio-based vegetation indices, the unadjusted indices (SR and NDVI) performed best because our soil line was not substantially different from that assumed by these indices. As a result, for the soil-adjusted indices, TSAVI, which used a site specific soil line, explained more variability in vegetation cover than other soil-adjusted indices. Indices that incorporated larger soil line adjustments explained progressively less variation. GVI explained substantially less variability, possibly because of the influence of substrate variability on middle infrared bands. Bandwise multiple regression provided superior results to the use of indices because it allows the decoupling of individual bands and the potential for different band responses.

Although substantial success has been achieved through the use of vegetation indices to predict ecological variables, we believe that bandwise multiple regression should achieve equivalent or better results without additional effort. In order to understand the relationship between an index and an ecological variable of interest, it is usually necessary to perform regression or other analysis to establish the relationship. The use of vegetation indices unnecessarily constrains the regression analysis. Instead, we have shown that improved results may be obtained by performing regression on the original bands and using a range of regression techniques (stepwise analysis, individual band transformations, polynomial terms) to fit the best regression model.

Acknowledgments

The authors wish to acknowledge the assistance of Peter Frenzen and Gordon Glockner, Mount St. Helens National Volcanic Monument, Warren Cohen, U.S. Forest Service Pacific Northwest Research Station, and Thomas Erkert, Gifford Pinchot National Forest, for their support in this project. Warren Cohen and Frederick Swanson, U.S. Forest Service Pacific Northwest Research Station, Alfredo Huete, University of Arizona, and Steve Stehman, Syracuse University, provided constructive reviews of the manuscript. Partial funding for this project was provided through the National Science Foundation (grant #GER-9452810) under the auspices of the NSF Graduate Research Fellowship in Landscape Studies.

References

Anderson, G. L., Hanson, J. D., and Haas, R. H. (1993), Evaluating Landsat thematic mapper derived vegetation indices for estimating above-ground biomass on semiarid rangelands, *Remote Sensing of Environment* 45:165-175.

Baret, F., Guyot, G., and Major, D. (1989), TSAVI: a vegetation index which minimizes soil brightness effects on LAI of APAR estimation, in *12th Canadian Symposium on Remote Sensing and IGARSS'90*, Vancouver, Canada, 10-14 July, 4 pp.

Boyd, D. S., and Ripple, W. J. (1997), Potential vegetation indices for determining global forest cover, *International Journal of Remote Sensing* 18:1395-1401.

Chen, J. M., and Cihlar, J. (1996), Retrieving leaf area index of boreal conifer forests using Landsat TM images, *Remote Sensing of Environment* 55:153-162.

Cihlar, J., St.-Laurent, L., and Dyer, J. A. (1991), Relation between the normalized difference vegetation index and ecological variables, *Remote Sensing of Environment* 35:279-298.

Crist, E. P., and Cicone, R. C. (1984), Application of the Tasseled Cap concept to simulated Thematic Mapper data, *Photogrammetric Engineering and Remote Sensing* 50:343-352.

del Moral, R., and Bliss, L. C. (1993), Mechanisms of primary succession: insights resulting from the eruption of Mount St. Helens, In *Advances in Ecological Research*, vol. 24 (M. Began and A. H. Fitter, Eds.), Academic Press, London, pp. 1-65.

Dusek, D. A., Jackson, R. D., and Musick, J. T. (1985), Winter wheat vegetation indices calculated from combinations of seven spectral bands, *Remote Sensing of Environment* 18:255-267.

Elvidge, C. D., and Lyon, R. J. P. (1985), Influence of rock-soil spectral variation on assessment of green biomass, *Remote Sensing of Environment* 17:265-279.

ERDAS (1995), *ERDAS Field Guide*, 3rd ed., ERDAS, Inc, Atlanta, GA, 628 p.

Franklin, J. F., Frenzen, P. M., and Swanson, F. J. (1988), Re-creation of ecosystems at Mount St. Helens--contrasts in artificial and natural approaches, In *Rehabilitating Damaged Ecosystems* (J. Cairns, Ed.), CRC Press, Boca Raton, FL., pp. 1-37.

Franklin, J. F., MacMahon, J. A., Swanson, F. J., and Sedell, J. R. (1985), Ecosystem responses to the eruption of Mount St. Helens, *National Geographic Research* 1:198-216.

Frenzen, P. (1992), Mount St. Helens: a laboratory for research and education, *Journal of Forestry*, 90:14-18, 37.

Frenzen, P. M., Delano, A. M., and Crisafulli, C. M., comps. (1994), *Mount St. Helens: Biological Responses Following the 1980 Eruptions -- An Indexed Bibliography and Research Abstracts (1980-93)*, Gen. Tech. Rep. PNW-GTR-342, Portland, OR: U.S. Department of Agriculture, Forest Service, Pacific Northwest Research Station, 149 p.

Friedl, M. A., Davis, F. W., Michaelsen, J., and Moritz, M. A. (1995), Scaling and uncertainty in the relationship between the NDVI and land surface biophysical variables: an analysis using a scene simulation model and data from FIFE, *Remote Sensing of Environment* 54:233-246.

Hoblitt, R. P., Miller, C. D., and Vallance, J. W. (1981), Origin and stratigraphy of the deposit produced by the May 18 directed blast, In The 1980 Eruptions of Mount

St. Helens, Washington (Lipman, P. W., and Mullineaux, D. R., Eds), U.S. Government Printing Office, Washington, D. C., pp. 401-419

Huete, A. R. (1988), A soil-adjusted vegetation index (SAVI), *Remote Sensing of Environment* 29:295-309.

Huete, A. R., and Jackson, R. D. (1988), Soil and atmosphere influences on the spectra of partial canopies, *Remote Sensing of Environment* 25:89-105.

Jordan, C. F. (1969), Derivation of leaf-area index from quality of light on the forest floor, *Ecology*, 50:663-666.

Kauth, R. J., and Thomas, G. S. (1976), The Tasselled Cap – a graphic description of the spectral-temporal development of agricultural crops as seen by Landsat, In *Proceedings of the symposium on Machine Processing of Remotely Sensed Data*, Purdue University, West Lafayette, IN. pp. 51-51.

Lillesand, T. M., and Kiefer, R. W. (1994), *Remote Sensing and Interpretation*, 3rd ed., John Wiley & Sons, Inc., New York, 750 p.

Lipman, P. W., and Mullineaux, D. R., eds. (1981), *The 1980 Eruptions of Mount St. Helens, Washington*, U.S. Government Printing Office, Washington, D. C., 844 p.

Markham, B. L., and Barker, J. L. (1986), Landsat MSS and TM post-calibration dynamic ranges, exoatmospheric reflectances and at-satellite temperatures, *Landsat Technical Notes* 1:3-8.

Montgomery, D. C. (1991), *Design and Analysis of Experiments*, 3rd ed., New York, John Wiley & Sons, 649 p.

Myneni, R. B., and Williams, D. L. (1994), On the relationship between FAPAR and NDVI, *Remote Sensing of Environment* 49:200-211.

Perry, C. R., and Lautenschlager, L. F. (1984), Functional equivalence of spectral vegetation indices, *Remote Sensing of Environment* 14:169-182.

Qi, J., Chehbouni, A., Huete, A. R., Kerr, Y. H., and Sorooshian, S. (1994), A modified soil adjusted vegetation index, *Remote Sensing of Environment* 48:119-126.

Ripple, W. J. (1985), Asymptotic reflectance characteristics of grass vegetation, *Photogrammetric Engineering and Remote Sensing* 51:1915-1921.

Ripple, W. J. (1994), Determining coniferous forest cover and forest fragmentation with NOAA-9 Advanced Very High Resolution Radiometer data, *Photogrammetric Engineering & Remote Sensing* 60:533-540.

Rondeaux, G., Steven, M., and Baret, F. (1996), Optimization of soil-adjusted vegetation indices, *Remote Sensing of Environment* 55:95-107.

Rouse, J. W., Haas, R. H., Schell, J. A., Deering, D. W., and Harlan, J. C. (1973), Monitoring the vernal advancement and retrogradation (greenwave effect) of natural vegetation, NASA/GSFC Type III Final Report, Greenbelt, Maryland.

Running, S. W., Peterson, D. L., Spanner, M. A., and Teuber, K. B. (1986), Remote sensing of coniferous forest leaf area, *Ecology*, 67:273-276.

Spanner, M. A., Pierce, L. L., Running, S. W., and Peterson, D. L. (1990), The seasonality of AVHRR data of temperate coniferous forests: relationship with leaf area index, *Remote Sensing of Environment*, 33:97-112.

Tucker, C. J. (1979), Red and photographic infrared linear combinations for monitoring vegetation, *Remote Sensing of Environment* 8:127-150.

Ugolini, F. C., Dahlgren, R., LaManna, J, Nuhn, W., and Zachara, J. (1991), Mineralogy and weathering processes in Recent and Holocene tephra deposits of the Pacific Northwest, USA, *Geoderma*, 51:277-199.

Wiegand, C. L., Richardson, A. J., Escobar, D. E., and Gerbermann, A. H. (1991), Vegetation indices in crop assessments, *Remote Sensing of Environment* 35:105-119.

Yoder, B. J., and Waring, R. H. (1994), The normalized difference vegetation index of small Douglas-fir canopies with varying chlorophyll concentrations, *Remote Sensing of Environment* 49:81-91.

Chapter 3. Use of Growth Curves to Characterize Succession with Multitemporal Satellite Imagery: Mount St. Helens 1980-1995

Rick L. Lawrence and William J. Ripple

Forest Resources Department,
Oregon State University,
Corvallis, Oregon,
January 14, 1998.

Abstract

We developed and tested a method for analyzing multitemporal satellite imagery using growth curves. The method is flexible and allows an analyst to extract specific change parameters from the curves depending on the research question of interest. Eight satellite images of the Mount St. Helens blast zone from 1984 to 1995 were geometrically and radiometrically corrected. They were then transformed to estimates of green vegetation cover. Unsupervised clustering was performed on the set of eight transformed images and polynomial growth curves were fit to the cluster means. From these fitted curves, parameters of interest were extracted and returned to GIS layers, including number of years to reach 10% cover, the greatest rate of cover increase during the study period, and time-integrated cover. Statistical analysis indicated that the curves did a good job of representing the growth trajectories of unclustered pixels. We demonstrated the use of growth curve analysis by analyzing the importance in the revegetation of Mount St. Helens of the different types of disturbance resulting from the volcanic eruption. The growth curve analysis is useful in a variety of applications where the data are continuous, more than two dates of data are available, and the underlying question of interest relates to trends in the data.

Introduction

The recovery of vegetation following the 1980 eruption of Mount St. Helens has been one of the great ecological stories of the Pacific Northwest during the past two decades. From a 550 square kilometer homogeneous "moonscape" following the eruption on May 18, 1980, to a heterogeneous landscape that includes areas of lush vegetation today, the story of Mount St. Helens' recovery is unfolding in many ways. The study reported in this paper presents one way of reading this story, using a series of satellite images to characterize vegetation changes since 1980.

Analysis of vegetation change over time has become one of the most important uses of satellite remote sensing of natural resources (Lillesand and Kiefer, 1994; Coppin and Bauer, 1996). Although a wide variety of techniques has been used to analyze vegetation change using satellite imagery (*e.g.*, Muchoney and Haack, 1994), much of the research has focussed on year-to-year changes, rather than trends. Coppin and Bauer (1996) reviewed change detection techniques and listed 11 general approaches. Of these approaches, one is based on a single date of imagery, eight are based on year-to-year changes, and two (composite analysis and multitemporal linear data transformation) can be applied to three or more dates. Even when long time series have been used, the ecological analysis often focuses on year-to-year changes (e.g., Lambin and Strahler, 1994; Olsson, 1994; Eastman and Fulk, 1993).

Vegetation change profiles derived from satellite imagery have been used previously for several purposes. Several studies examining seasonal vegetation change have used vegetation profiles based on more than two images to differentiate growing conditions among sites (Peterson, 1992), distinguish land cover types (Samson, 1993), and compare differences in vegetation types as well as year-to-year phenologic variability (Reed et al., 1994). In addition, reflectance trajectories of forest stands of different ages have been calculated to show change in reflectance associated with succession (Peterson and Nilson, 1993).

Examination of the shape of growth trajectories has been recognized in various natural resource fields as being important in understanding ecosystem responses. This has been true in studies of plant community responses. For example, Halpern and Franklin (1990) compared response curves in Douglas-fir forests as a function of disturbance intensity and stand history. Similarly, Armesto and Pickett (1986) compared vegetation growth curves in abandoned fields to test theories of different successional mechanisms. At Mount St. Helens, both del Moral and Bliss (1993) and Halpern et al. (1990) have used vegetation growth trajectories to compare recovery across diverse growing conditions created by the eruption. These studies have generally not quantified the difference in the shapes of vegetation growth curves, but they have recognized that the trajectory an ecosystem takes to achieve a given stand condition reveals important information about how the ecosystem operates. For example, two ecosystems might each start a time series with 10% cover and end with 80% cover. However, if the first system traveled an asymptotic path to 80% cover and the second traveled a path of geometric increases, then the mechanisms controlling vegetation changes probably differed. Further, projected future conditions for each system might be vastly different.

Rigorous mathematical characterization of plant growth curves has long been central to biometric studies (Hunt, 1982). This approach has commonly been applied at both the individual plant and stand level to characterize change in vegetation amount, whether measured as tree height, bole volume, stand basal area, canopy closure, or any number of other measures. Applications have included complex theoretical growth functions for empirical applications (Richards, 1959), site-index curves (Heger, 1968), and many others. Empirical forest growth models used for stand prediction and economic modeling are generally based on empirically derived plant growth curves.

The objective of our research was to develop and test a method for characterizing vegetation change at Mount St. Helens since the eruption in 1980 using growth curves. The theoretical basis for this research was the same as presented in plant community and biometric studies. Thus, we assumed that (1) vegetation growth trajectories vary spatially across the Mount St. Helens blast zone and (2) these patterns have ecological explanations and significance. The first assumption is tested by our application of the procedure we present for determining growth curves. Although we present one example in this paper of how the second assumption might be tested, the next stage of our research will test this assumption in detail when we attempt to explain observed patterns in the curves using ecological variables.

Study Area

The 1980 eruptions of Mount St. Helens may be the most documented volcanic eruptions in history. In one sense, the May 18 eruption has been viewed as a single catastrophic event. However, for most ecological purposes it is best viewed as a related suite of volcanic and hydrologic disturbance events that resulted in a complex mosaic of disturbed patches. Although minute-by-minute accounts of the events have been presented (e.g., Lipman and Mullineaux, 1981), one paragraph by Franklin et al. (1985:201) provides a thumb-nail sketch:

> The 18 May 1980 eruption began at 0832 PDT when a large earthquake triggered a massive avalanche of debris involving the entire upper portion of the mountain. Movement of this mass unroofed the core of the mountain where superheated groundwater flashed to steam, unleashing a blast of steam and rock debris in a 180° arc to the north. Mudflows rampaged through the valley-bottom forests to the west and southeast. Volcanic ash rained from the sky to the northeast of the mountain from the morning of 18 May into the next day. In early afternoon of 18 May and during the subsequent eruptions, pumiceous pyroclastic flows (flows of hot gases and pumice) spilled northward out of the newly formed crater across the deposits left by the avalanche.

The effects were clearly devastating to much of the ecosystems throughout the affected area. Disturbed areas were generally well defined depending on the type of disturbance affecting them. Thus, the resulting landscape is a mosaic of deposits from the debris avalanche, pyroclastic flows, mudflows, downed timber, scorched vegetation, and airfall tephra. Each of these deposits has distinctive characteristics regarding thickness, deposit temperature, and substrate composition (Franklin et al., 1988). As a result, potential spectral properties of the substrate and potential rates of vegetative recovery vary significantly throughout the area.

The specific selection of our study area (Figure 4) was dictated by the larger study of which this research is a part. That larger study is examining the natural recovery of the area devastated by the 1980 eruptions. Therefore the study area was limited to that

Figure 4. Digital elevation model of the study area. The volcano crater is located in the lower center surrounded by mudflows radiating to the south, Spirit Lake is east of center, and the Toutle River drainage extends to the west.

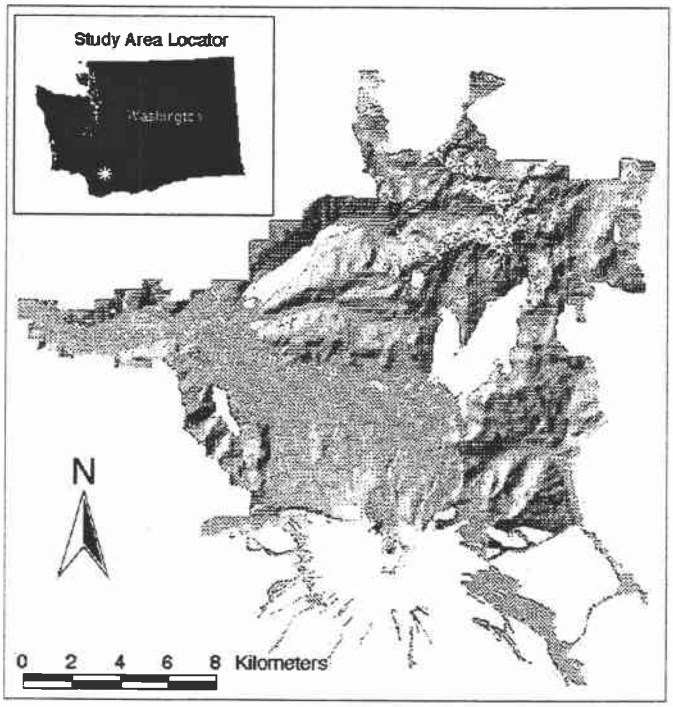

portion of the devastated area that has not been replanted to trees following the eruption. Large water bodies within the area were also excluded. The study area consisted of approximately 25,400 hectares, or approximately 42% of the area devastated by the eruption.

Vegetation structure and types are not readily summarized for the study area because plant cover is highly variable, within-site plant diversity is often high, and successional changes are, in some cases, rapid, making previous reports rapidly dated. Early reports of vegetation in blowndown forests reported 0.2% mean canopy cover in 1981, with dominant species primarily herbaceous, including pearly everlasting (*Anaphailis margaritacea)*, thistle (*Cirsium* spp.), fireweed (*Epilobium* spp.), ryegrass (*Lolium* spp.), and groundsel (*Senecio* spp.) (Franklin, et al., 1985). By 1992, these species had completely covered portions of the landscape (Frenzen, 1992). In subalpine study sites, substantially different patterns have been reported (del Moral and Bliss, 1993). Recovery has varied depending on the nature of the disturbance, with less than 1% cover reported on pyroclastic flows, under 5% on mudflows, and over 40% on adjacent tephra covered sites. Although there is significant overlap in species composition among these sites, dominance varies greatly. In 1990, the most abundant species on subalpine tephra sites included, in order of importance, bentgrass (*Agrostis diegoensis),* prairie lupine (*Lupinus lepidus*), spreading phlox (*Phlox diffusa*), and Newberry fleeceflower (*Polygonum newberryi*), and on a subalpine mudflow Newberry fleeceflower, prairie lupine, and Cardwell's penstemon (*Penstemon cardwellii*). However, there was significant change in the relative importance of species on the mudflow site between 1988 and 1990, emphasizing the rapid changes taking place within the area. Although tree species are not yet of significant influence within the Mount St. Helens devastated area, in some areas late snow banks at the time of the eruption protected mountain hemlock (*Tsuga mertensiana*) and Pacific silver fir (*Abies amabilis*). Scattered alder (*Alnus* spp.) and Douglas-fir (*Pseudotsuga menziesii*) have appeared throughout the area, and some roots of willows (*Salix* spp.) and black cottonwood (*Populus trichocarpa*) that were up-rooted by mudflows and the debris avalanche happened to come to rest at the surface and resprout (Frenzen, 1992).

Methods

Data Acquisition

We acquired eight dates of Landsat Thematic Mapper (TM) images of our study area (path 46, row 28): 19 July 1984; 26 August 1986; 31 August 1988; 9 September 1991; 10 August 1992; 29 August 1993; 31 July 1994; and 19 August 1995. Three GIS layers were used for this study, including the boundary of Mount St. Helens National Volcanic Monument (the Monument) and a forest stand data layer, each provided by the Gifford Pinchot National Forest, and a layer detailing the types of disturbance resulting from the volcanic eruptions, which was manually digitized from a map prepared by the USGS (Lipman and Mullineaux, 1981).

Preprocessing

All images were geometrically rectified to the 1991 scene, which we received georeferenced to a Universal Transverse Mercator (UTM) grid. For each rectification, 10 to 30 ground control points were used, and total root mean square errors ranged from 0.278 to 0.432. Images were geometrically transformed using nearest neighbor resampling to a 25 meter pixel size.

Following geometric rectification, all images were radiometrically normalized to the 1995 image using the matched digital counts method described by Collins and Woodcock (1996). We located 30 colocatable points of invariate features, 10 in each of three cover types, water, mature forest, and bare soil. Of these 30 points, 18 (six for each cover type) were randomly selected to calibrate regression equations, in each case predicting 1995 digital numbers for each spectral band used in the study for each year of imagery. The 12 colocatable points not used to calibrate the regression equations were used for independent verification of the equations. For each independent verification point, on a year-by-year, band-by-band basis, the squared error between the regression equation predicted values and the actual 1995 values were compared to confirm that the regression equations improved the radiometric match with the 1995 image. Radiometric correction equations were used only when they improved the radiometric match based on the independent verification points.

The images for each date were subset using a single mask created from GIS layers. These layers were used to delineate portions of the Mount St. Helens blast zone that had not been replanted to trees following the eruption. In addition, large water bodies, areas of snow within the 1995 image, and areas of fog within the 1984 image were masked.

Finally, the images for each year were converted to spectrally estimated percent of green vegetation cover (Estimated Cover) (Figure 5), based on a regression formula developed with the 1995 image (Lawrence and Ripple, in press). The regression formula, which was found to predict Estimated Cover better than vegetation indices, was based on the relationship between the 1995 image spectral response and percent green vegetation cover, as estimated from aerial photographs. The relevant formula was:

$$\text{Estimated Cover} = 106.00 - 5.50\, B_{RED} + 0.048\, B_{RED}^2 + 1.36\, B_{NIR} - 0.0051\, B_{NIR}^2$$

where: Estimated Cover = percent of pixel covered by green vegetation as estimated by spectral bands

B_{RED} = red band (Landsat TM band 3) digital value

B_{NIR} = near infrared band (Landsat TM band 4) digital value

The model was highly significant (p-value < 0.0001), and the multiple R^2 was 0.75.

Figure 5. Spectrally estimated vegetation cover for each of the images used in the study. A regression formula was used to transform Landsat TM images to an estimate of percent green vegetation cover for each pixel.

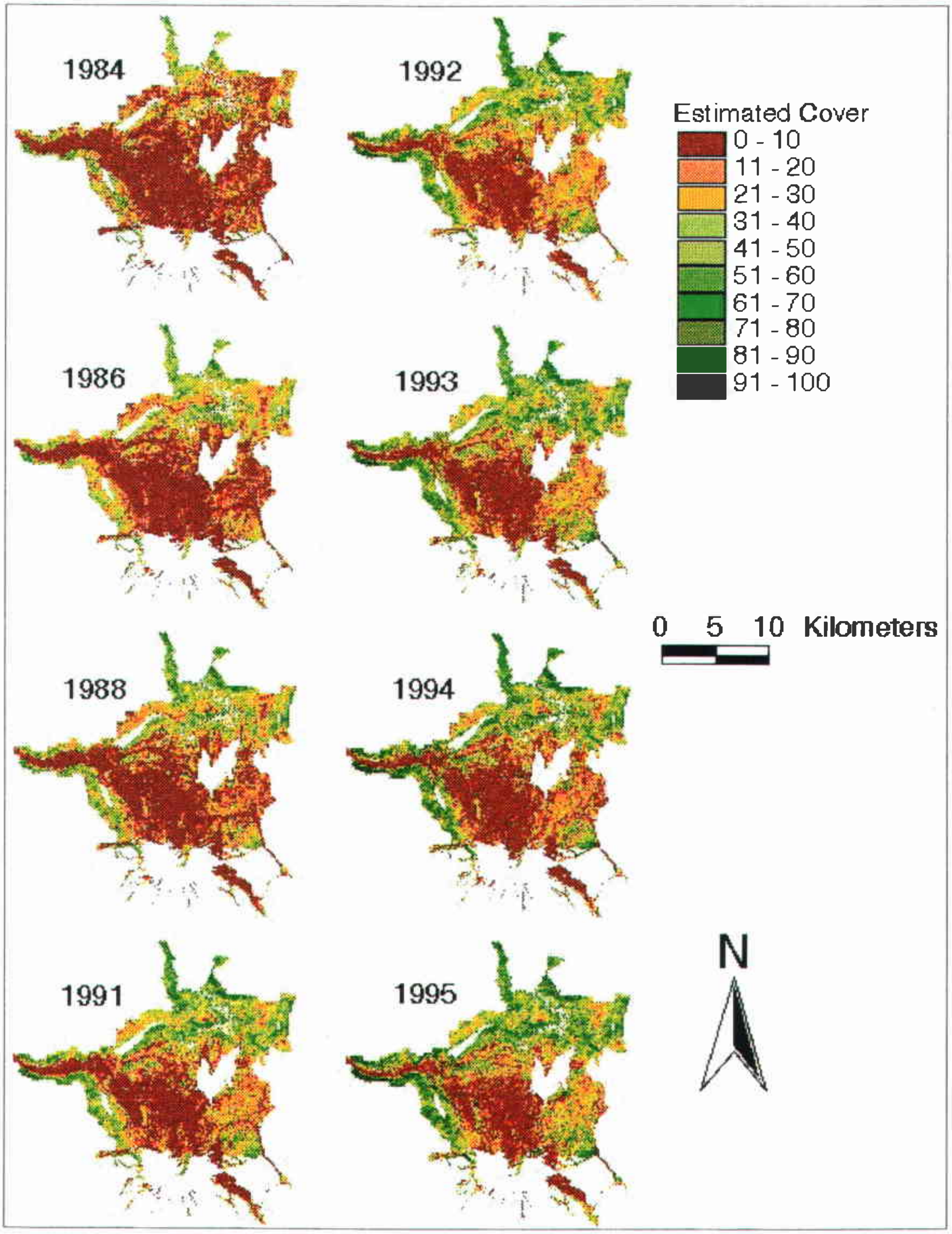

Growth Curve Fitting

Growth models may be linear or non-linear in their parameters. For linear models, such as polynomials, least squares fits can be readily computed. For non-linear models having more than one parameter, all parameters except the parameter of interest can be estimated and the parameter of interest can be computed (Richards, 1959). The study area contains over 400,000 pixels (25 m by 25 m). Therefore, to fit a growth curve on a pixel-by-pixel basis requires 400,000 curve fits. This was impractical for non-linear growth models, where certain parameters must be estimated based on some *a priori* knowledge, and would be computationally intensive for linear models. Therefore, we needed a way to reduce the number of curves to fit.

Unsupervised statistical clustering of the eight Estimated Cover images created clusters that were distinguished by the Estimated Cover trajectories (and, presumably, their vegetation growth curves). The clustering occurred in an eight-dimension feature space where the axes were the years and the data were the Estimated Cover values. Thus, for example, pixels that had low values in all eight years clustered separately from pixels that began with low values and increased to high values geometrically. Generally, clusters were distinguishable by magnitude of Estimated Cover values (vegetation amount), rates of change, and growth curve shape (e.g., straight line, geometric curve, asymptotic, sigmoid).

The clustering was performed using the ISODATA command in ARC/Grid software. The number of clusters chosen was arbitrary, but we estimated, based on knowledge of the study area and a pilot study, that 20 to 30 clusters would allow adequate distinction of different amounts of vegetation and likely vegetation trajectories, while providing a small enough number of clusters for practical data analysis. Other ISODATA parameters that could be set in ARC/Grid were maximum number of iterations (20 were permitted) and minimum cluster size (1000 pixels were specified).

A reasonable estimate of non-linear parameters was not available. As a result, a linear model was used to fit growth curves. For each cluster resulting from the ISODATA procedure, the cluster means for each year were transferred to an S-Plus data frame (MathSoft, 1995). The S-Plus linear regression model was used to fit a series of polynomials (first, second, and third order) to the means of each cluster, with the growing season following the eruption as the independent variable. These models were expressed as:

First order polynomial: $\mu = \beta_0 + \beta_1 X$

Second order polynomial: $\mu = \beta_0 + \beta_1 X + \beta_2 X^2$

Third order polynomial: $\mu = \beta_0 + \beta_1 X + \beta_2 X^2 + \beta_3 X^3$

where μ was the mean Estimated Cover value, β_0 was the estimated intercept, β_i ($i = 0$ to 3) were estimated coefficients, and X was the growing season since the eruption (season 1 was prior to the first growing season). We assumed vegetation cover was 0% immediately following the eruption and prior to the first growing season, and assigned an Estimated Cover value of 0 to all pixels for season 1.

For each cluster, the addition of each polynomial term was tested using an extra-sum-of-squares F-test, and higher order terms were only included if the p-value for the added term was less than 0.10. Although other tests can be used to chose the best fitting polynomial, using the F-test is the most conservative (least likely to add terms), especially where there are a limited number of observations (in this case, nine observations, eight per cluster plus season 1) (Hunt, 1982).

The fitted growth curves were tested to determine whether they adequately represented the original pixel values. We randomly selected 100 pixels from the study area. For the random pixels we computed (1) the average Estimated Cover for the eight image dates prior to clustering and curve fitting and (2) the average Estimated Cover predicted by the fitted growth curves for the same dates. These two sets of values were compared using a paired T-test.

We extracted three parameters from the growth curves to illustrate the utility of this change detection method. The parameters extracted included:

(1) number of years the curve took to reach an Estimated Cover of 10%, expressed as

$$\rho_1 = \beta_0 + \beta_1 X + \beta_2 X^2 + \beta_3 X^3 - 10$$

where ρ_1 = number of years to reach 10% Estimated Cover;

(2) the greatest rate of Estimated Cover increase (maximum first derivative) during the study period, expressed as

$$\rho_2 = \max[d\mu/dX] = \max[\beta_1 + 2\beta_2 X + 3\beta_3 X^2]$$

where ρ_2 = the maximum first derivative of μ with respect to X; and

(3) time-integrated Estimated Cover, as determined by the area under the curve (integral) during the study period, expressed as

$$\rho_3 = \int(\beta_0 + \beta_1 X_i + \beta_2 X_i^2 + \beta_3 X_i^3)$$

where ρ_3 = the integral of μ with respect to X_i (i = 1 to 17).

To extract the parameters listed above, we entered the curve intercepts and coefficients into a spreadsheet and wrote three simple macros in Visual Basic to (1) solve each curve for Estimated Cover equal to 10 (the solution is in growing seasons after the eruption), (2) determine the maximum first derivative of each curve (in Estimated Cover per year), and (3) integrate the curve to determine the area under the curve (in units of integrated Estimated Cover, with possible values from 0 to 1600).

The results of the parameter determination were used to recode the clustered image. For example, the fitted curve for one of the clusters was:

$$\text{Estimated Cover} = -17.6 + 20.4\,X - 1.8\,X^2 + 0.05\,X^3$$

where X = number of growing seasons after the eruption. A plot of this growth curve is shown in Figure 6 (curve D4). This curve increases rapidly in early years and then becomes asymptotic. The number of growing seasons to reach 10% Estimated Cover was 1.5, the greatest rate of curve increase is an increase in Estimated Cover of 17% for each growing season, and time-integrated Estimated Cover was 827. Each of these values was transferred to a separate GIS layer, along with corresponding values for each of the other clusters and their associated growth curves (Figures 7(a), (b), and (c)).

Figure 6. Growth curves fitted to 24 cluster means resulting from multitemporal clustering of the eight Estimated Cover layers in Figure 5. The axes are the same for each graph. The X axis represents the growing seasons from 1 (prior to the first growing season after the eruption) to 17 (1995). The Y axis represents Estimated Cover from 0 to 100.

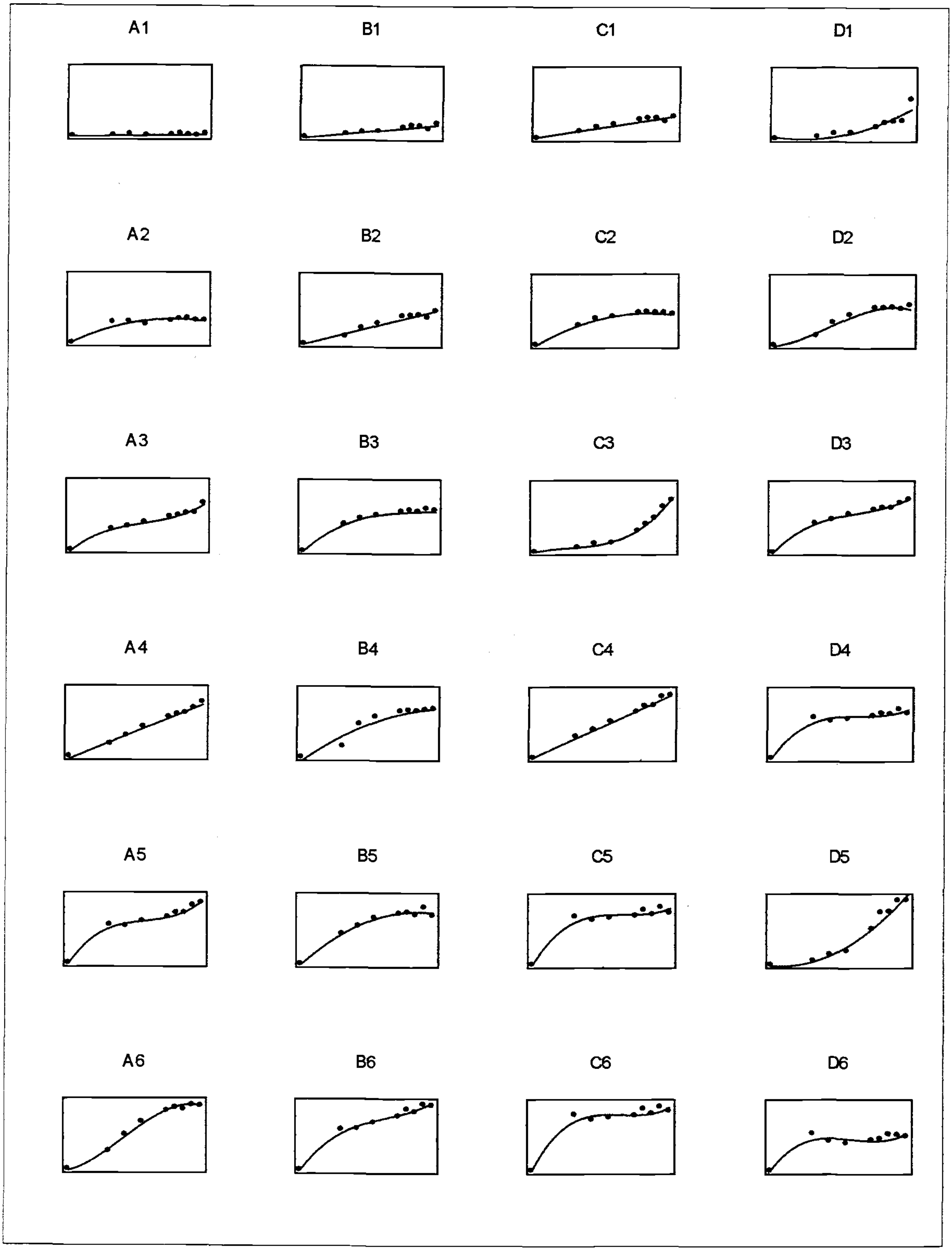

Demonstration of Use of Growth Curves

To demonstrate the utility of, and further test, the method, we applied our analysis to a specific ecological question. Previous plot-based research has noted a relationship between revegetation at Mount St. Helens and the nature of the disturbance resulting from the volcanic eruption (del Moral and Bliss, 1993; Means et al., 1982). Volcanic deposits varied greatly as to thickness and temperature (Franklin et al., 1985). The debris avalanche and mudflows were less than 100°C, the tree blowdown and scorched areas ranged from 100° to 350°C, and the pyroclastic flows were 350° to 850°C. The debris avalanche was 10m to over 100m thick, the pyroclastic flows were 1m to 10m thick, deposits from mudflows and in the tree down areas were about 0.1m to 1m thick, and deposits in the scorched tree areas were less than 0.1m thick.

These differences in volcanic deposits had significant effects on the presence of surviving rootstock, the ability of such survivors to resprout above ground, and the ability of germinating seeds to reach organic soils. We believed that these effects should be observable with our analysis. Further, we hypothesized that the nature of these effects would vary depending on how revegetation was measured. For example, we expected that the greater depth of deposits in the tree-down area, as compared to the scorched tree area, would result in slower early recovery and longer times to reach 10% cover in the tree-down area. However, toward the end of our study period the vegetation growth curves in these two areas were, in many cases, becoming asymptotic. As a result, we expected less difference between in these areas for measures of ending vegetation or maximum rates of increase.

To test this hypothesis, we created a GIS layer showing six types of volcanic disturbance, pyroclastic flows, mudflows, debris avalanche, tree removal, tree blowdown, and scorched trees (Figure 7(d)). For 500 random points, we then extracted four measures of vegetation response (time to reach 10% Estimated Cover, greatest rate of Estimated Cover increase, time-integrated Estimated Cover, and 1995 Estimated Cover), which were each regressed against type of disturbance using simple linear regression.

Figure 7. GIS layers resulting from the extraction of three parameters from the fitted growth curves and disturbance type layer. Years to 10% Cover was obtained by solving the curve for 10. Rate of Estimated Cover Increase was obtained by finding the maximum value of the curve's first derivative during the study period. Time-integrated Estimated Cover was obtained by integrating the curve over the study period.

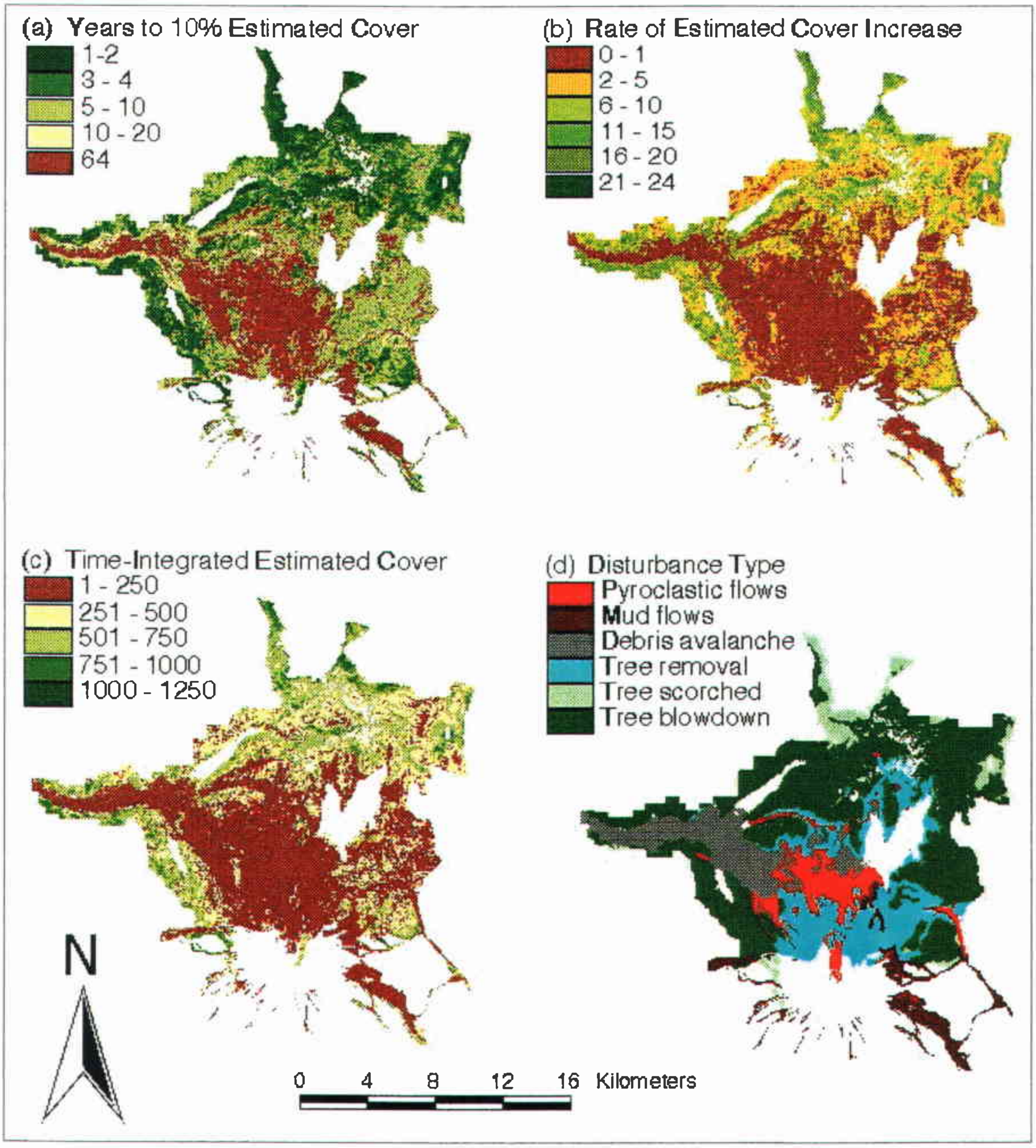

Results

The clustering procedure resulted in 24 clusters representing different vegetation growth trajectories (Figure 6). (References to specific curves in this paper refer to the designations in Figure 6.) We extracted intercepts, coefficients, model p-values, and model R^2s for each of the curves (Table 6). A co-occurrence matrix for the curves and types of disturbance enabled us to describe, qualitatively, the spatial extent of the clusters represented by the curves with respect to the volcanic disturbances (Table 7).

Table 6. Statistics for growth curves fitted to means of multitemporal clusters. Curve designations are from Figure 6. P-values indicate that all models are highly significant, except for Curve A1, which is marginally significant. R^2 values indicate the percentage of variation in cluster means explained by the fitted curves.

Curve Designation	β_0 (Intercept)	β_1 (X coefficient)	β_2 (X^2 coefficient)	β_3 (X^3 coefficient)	p-value	R^2
A1	0.22	0.16	--	--	0.09	0.36
B1	-1.32	1.13	--	--	<0.001	0.89
C1	-0.30	1.89	--	--	<0.001	0.93
D1	4.65	-2.34	0.27	--	0.004	0.84
A2	-3.35	5.85	-0.22	--	<0.001	0.90
B2	-2.51	3.00	--	--	<0.001	0.95
C2	-7.50	7.64	-0.27	--	<0.001	1.00
D2	-1.65	0.21	0.72	-0.03	<0.001	0.98
A3	-10.45	11.29	-0.96	0.03	<0.001	0.99
B3	-11.34	12.13	-0.73	0.02	<0.001	1.00
C3	-3.01	3.51	-0.52	0.03	<0.001	1.00
D3	-13.66	14.8	-1.15	0.03	<0.001	1.00
A4	-7.73	4.91	--	--	<0.001	0.99
B4	-13.06	8.82	-0.23	--	<0.001	0.93
C4	-4.38	5.62	--	--	<0.001	0.99
D4	-17.63	20.38	-1.76	0.05	<0.001	0.96
A5	-18.53	20.94	-1.91	0.06	<0.001	0.99
B5	-11.30	11.52	-0.38	--	<0.001	0.98
C5	-21.00	24.21	-2.07	0.06	<0.001	0.95
D5	0.78	-2.06	0.47	--	<0.001	0.98
A6	-2.45	0.73	1.07	-0.05	<0.001	0.99
B6	-16.31	18.39	-1.35	0.04	<0.001	0.98
C6	-24.78	28.60	-2.52	0.07	<0.001	0.96
D6	-16.79	20.14	-2.01	0.06	0.007	0.90

Table 7. Spatial extent of clusters relative to their fitted curves and the volcanic disturbance. Curve designations are from Figure 6.

Curve Designation	Area (hectares)	Spatial Extent Relative to Volcanic Disturbance
A1	6976	Pyroclastic flows and large portions of debris avalanche, and mudflows
B1	4551	Pyroclastic flows, debris avalanche, and mudflows
C1	2809	Tree blowdown and tree removal
D1	1051	Debris avalanche and mudflows
A2	1246	Scattered locations in tree blowdown and tree removal
B2	1711	Primarily in tree blowdown
C2	983	Scattered in tree blowdown and tree scorched
D2	697	Primarily in tree blowdown
A3	493	Primarily in tree blowdown
B3	798	Scattered in tree blowdown and tree scorched
C3	432	At edges of debris avalanche and mudflows
D3	458	Scattered in tree blowdown and tree scorched
A4	298	Scattered in tree blowdown and tree scorched
B4	278	Scattered in tree blowdown and tree scorched
C4	175	Primarily in tree blowdown
D4	403	Primarily in tree scorched
A5	207	Scattered in tree blowdown and tree scorched
B5	200	Scattered in tree blowdown and tree scorched
C5	169	Scattered in tree blowdown and tree scorched
D5	139	At edges of debris avalanche
A6	97	In tree blowdown and tree scorched in Toutle River Valley
B6	149	In tree blowdown and tree scorched in Toutle River Valley
C6	110	In tree scorched and at edges of mudflows
D6	475	Scattered in tree blowdown and tree removal areas

With one exception (curve A1), all polynomial curves fit to the cluster means were highly significant (all p-values < 0.007) and explained between 84% and 100% of the variability in the cluster means. Curve A1 was marginally significant (p-value = 0.09) and explained only 36% of the variability. This cluster represented areas of very low variation throughout the study period. Of the 24 fitted polynomial curves, six were first order, six were second order, and 12 were third order.

Our test of the difference between pixel-level estimates of vegetation cover and estimates of vegetation cover from the growth curves indicated how well the growth curves reflected the response of pixels prior to clustering and curve fitting. The paired T-test estimated values for the unfitted pixels at 0.5% less than the growth curve estimates, with a 95% confidence interval from -1.2% to 0.2%. We believe the 0.5% difference is ecologically insignificant. The inclusion of 0 in the confidence interval indicates that, statistically, there was no difference between the original pixels and the values estimated by the growth curves. Thus, there was convincing statistical evidence that the growth curves did a good job of reflecting the response of the original pixels.

Specific parameters from the growth curves were extracted (Table 8) and used to reclassify the clusters resulting from the multivariate clustering (Figure 7). The layer representing an estimate of how many years each pixel took to reach 10% Estimated Cover (Figure 7(a)) provided us with significant additional information about the early response of vegetation that was not available from an analysis of only two dates. Although there was a substantial relationship between early vegetation response and total vegetation cover at the end of the study period, some areas showed significant variation from this pattern. For example, although both curves D1 and B2 (Figure 6) represented areas where Estimated Cover reached between 40% and 50% by the end of the study period, the early response was very different. Curve D1 had a very slow early response, requiring approximately 11 years to reach 10% Estimated Cover, but was increasing very rapidly at the end of the study period. In contrast, curve B2 had a more rapid early response, reaching 10% in only 4 years, and continued at a steady rate of increase at the end of the period. Throughout the study area, the number of years to reach 10% Estimated Cover varied from slightly over 1 year to almost 11 years. In addition, curve A1 did not reach 10% by the end of the study period. When we used time to reach 10% Estimated Cover as a response variable, type of volcanic disturbance was highly significant (p-value < 0.0001). The amount of variation in the response variable explained (R^2) was 40%.

Table 8. Parameters extracted from growth curves. Curve designations are from Figure 6. Years to Reach 10% Estimated Cover was obtained by solving the curve for 10. Time-integrated Estimated Cover was obtained by integrating the curve over the study period. Greatest Rate of Estimated Cover Increase was obtained by finding the maximum value of the curve's first derivative during the study period.

Curve Designation	Years to Reach 10% Estimated Cover	Time-Integrated Estimated Cover	Greatest Rate of Estimated Cover Increase
A1	64.0	26	0.2
B1	10.1	141	1.1
C1	5.5	265	1.9
D1	10.5	177	6.8
A2	2.5	422	5.4
B2	4.2	383	3.0
C2	2.5	542	7.1
D2	4.3	520	5.7
A3	2.2	568	9.5
B3	1.9	692	10.7
C3	8.2	326	15.9
D3	1.8	749	12.6
A4	3.6	579	4.9
B4	2.8	689	8.4
C4	2.5	735	5.6
D4	1.5	827	17.0
A5	1.5	881	17.3
B5	1.9	845	10.8
C5	1.4	982	20.2
D5	7.1	486	14.0
A6	3.3	839	8.9
B6	1.6	980	15.8
C6	1.3	1121	23.8
D6	1.5	658	16.3

The greatest rate of increase in Estimated Cover experienced by the curve during the study period was measured by the largest first derivative of the curve during the period (Figure 7(b)). Returning to our example above, curve B2 increased at a rate of about 3% Estimated Cover per year constant throughout the entire study period. However, curve D1 started at a much slower rate and, by the end of the study period, was increasing at a rate of almost 7% Estimated Cover per year. Maximum rates of increase for the entire study area ranged from almost flat (less than 0.2% increase per year) to almost 24% per year. Type of volcanic disturbance was also significant (p-value < 0.0001) as a predictor variable for maximum rate of increase. The amount of variation explained was 21%.

Integrating the curves over time represented an overall growth response during the study period. Again, this layer represented information that was not extractable from a two-date comparison. In the example discussed in the previous paragraphs, both curves started at 0% Estimated Cover and increased during the period to about 45% Estimated Cover. However, time-integrated Estimated Cover for curve B2 was over twice curve D1. For the entire study area, time-integrated Estimated Cover ranged from 26 to 1121. Using time-integrated Estimated Cover as a response variable, type of volcanic disturbance was still highly significant (p-value < 0.001). The amount of variability in time-integrated estimated cover explained by type of volcanic disturbance (R^2) was 37%. We also regressed the 1995 Estimated Cover values against type of volcanic disturbance. The results were highly significant (p-value < 0.0001), and the amount of variability in 1995 Estimated Cover values explained (R^2) was 33%.

Discussion

Our study showed that growth curve functions can be an effective tool in characterizing vegetation succession as mapped by digital imagery. We realized that the method we used (a combination of multivariate clustering and curve fitting) resulted in the loss of information from the original images because pixel values differed from their respective cluster means and the curve fits contained residual error. Both of these conditions can be expected in every application of this method. However, our results indicated that, at least for our study, this loss of information was not significant. The paired T-test comparing unfitted pixel values to curve estimates provided evidence that the curve fitting technique accurately represented the trajectories present in the original data.

We were concerned that the fit of curve A1, representing a large portion of the study area, was only marginally significant (p-value = 0.09) and had an R^2 of only 0.36. Our examination of the spatial extent of the pixels represented by this curve (Table 7) explained these results. This curve represented areas that were most severely affected by the eruption and that had little vegetative response as of the end of the study period (generally less than 5% cover). The vegetation in these areas consisted largely of annuals and sparse shrubs. We believe that, because of the sparse vegetation in this area and the slow rate of increase in cover, sources of annual variability not related to trends in vegetation change were stronger relative to overall vegetation trends than in other areas. These sources of variability might have included annual variability in soil moisture, uncorrected radiometric differences, annual climatic differences resulting in phenological variability, and differences each year in length of growing seasons prior to image acquisition. The overall trend was close to flat (an increase of less than 0.2% vegetation cover per year). Thus, these variations on a year-to-year basis were not readily modeled with growth curves, although the curve did represent the overall flat trend. Further, there was less variability in the data for curve A1 that could be explained by a fitted curve. Thus, in spite of the low percentage of variability explained, the residual standard error for curve A1 was less than 22 of the other 23 curves.

The growth curves (Figure 6) can be grouped into three major types, based on the types of disturbance where they primarily occur. The curves revealed much about the nature of revegetation in these areas. Generally, curves A1, B1, and C1 occurred on the pyroclastic flows, debris avalanche, tree removal and mudflows. These were areas most severely affected by the eruptions and in which essentially no surviving vegetation was present. All three of these curves were represented by first order polynomials that remain at low levels of cover by the end of the study period. Thus, the curves showed that these areas were establishing vegetation very slowly.

Curves D1, C3 and D5 occurred primarily at the edges of mudflows and the debris avalanche. Each of these curves was characterized by very slow increases in early years, with rapidly increasing rates of recovery toward the end of the study period. Many of these areas were characterized the establishment of alder, which took several years to establish, but which is now growing rapidly.

The remaining curves were found primarily in the tree blowdown and tree scorched areas, although they were also found to some extent in the tree removal areas. These curves were generally characterized by rapid increases in cover in early years, in many cases becoming asymptotic toward the end of the study period at approximately 50% to 80% Estimated Cover. We believe the shape of these curves reflected the effect of buried surviving vegetation and seeds that existed in much of these areas following the eruption. These survivors provided for rapid revegetation. However, factors such as substantial numbers of downed trees prevented these areas from becoming fully occupied. In addition, curves that represented a substantial amount of the tree removal areas (curves A2 and D6) generally became asymptotic at lower levels of cover than other areas.

The extensive field data necessary to conduct a validation of our results were not available because this study was conducted retrospectively. However, we were able to compare qualitatively some of our results with previously published trajectories from plot based studies at Mount St. Helens. Trajectories of percent mean cover from 1980 to 1990 have been published for plots in the scour, lahar, blast, Pumice Plains, and Plains of Abraham areas (del Moral and Bliss, 1993). The mudflow scour areas were primarily associated with our curve D1 (Table 7), while the other areas were primarily associated with curves A1 and B1. The plot based curves were consistent with our derived curves, with the scour area increasing to approximately 14% by 1990 in the plot based study and 15.5% by our study, and the other areas increasing very slowly to no more than 4% by 1990 in the plot based study and 2.1% in our study.

Similar trajectories have been published for 1980 to 1986 with respect to blown-down forest and scorched forest (Halpern et al., 1990). By 1986, both blown-down and scorched forest plots had between 10% and 15% cover. On a landscape scale, these areas have been noted to contain significant variability (Franklin et al., 1988). This is supported by our study, where 15 different growth curves are associated with these areas (Table 7). Although many of our curves associated with these areas predict greater vegetation cover than that shown in the plot based studies, the plot based results are within the range of our predicted values for blown-down and scorched forests.

The utility of this approach for change detection was demonstrated by our volcanic disturbance type analysis. As we expected, based on previous plot-level studies, vegetation recovery was significantly correlated to type of volcanic disturbance (all p-values < 0.001). There were, of course, many other factors that affected vegetation recovery as well. This resulted in a high level of significance for the correlation to type of disturbance, with only 20% to 40% of variance explained.

Although the significance of disturbance type could have been shown through other analyses, our growth curve analysis permitted us to make additional distinctions. While we expected that disturbance type would significantly affect revegetation throughout the study period, it was important to understand why the amount of variance explained varied with the measure of revegetation used.

The largest amount of variation explained (40%) was with respect to number of years to reach 10% Estimated Cover. This was a measure of early vegetation response. Previous studies noted the importance of surviving vegetation, especially below-ground portions of sprouting species, in the early response at Mount St. Helens (Franklin et al., 1985). We expected the presence of survivors would vary significantly with the type of disturbance and be reflected in the number of years to reach 10% cover. For example, in the tree scorched zone, above-ground vegetation was killed, but substantial below-ground vegetation should have survived beneath a relatively thin layer of fresh volcanic deposit. However, in the tree-down zone, the disturbance was more severe and deposits were somewhat thicker. In the debris avalanche and pyroclastic flow areas, deposits were too thick for spouting vegetation to penetrate, even if survivors existed. Compared to the debris avalanche, in the mudflows there was greater opportunity for uprooted plants to be deposited on or near the surface where they might resprout. These different mechanisms related to disturbance type strongly influenced early vegetation recovery and, as a result, disturbance type explained a large amount of variance in how fast an area responded.

Although statistically significant, type of disturbance only explained 33% of the variance in 1995 Estimated Cover. We believe that this occurred because other factors had increasing influence over revegetation with time. For example, in substantial portions of both the tree scorched and tree blowdown zones, Estimated Cover had become asymptotic by 1995 (Table 6, Figure 6). Thus, these areas became less distinguishable by disturbance type. Portions of the debris avalanche (especially those represented by curve D1), which in many cases did not reach 10% Estimated Cover for over 10 years, have now rapidly increased to 40% Estimated Cover or more, decreasing their distinction from portions of the tree blowdown zone. We believe that, in general, while the volcanic deposits dominated early recovery, over time other factors have played an increasing role in the variability of patterns across the Mount St. Helens landscape. These factors include an increasing influence of stochastic factors, such as seed dispersal by wind and climatic influences.

Type of disturbance explained the least amount of variance (21%) with respect to greatest rate of Estimated Cover increase. We believe that this variable responded to a more complex array of influences. The debris avalanche along the Toutle River Valley was an example. The central portion of this area had a very slow rate of recovery throughout the study period, possibly as a result of the continuing scouring effect of the

Toutle River in the active river channel that runs through this area. On the other hand, the edges of this area, after slow initial recovery, have experienced some of the greatest rates of increase in the entire study area with the establishment and growth of alder (*Almus* spp.). The pattern of recovery along the edges of the debris flow, with vegetation moving in from the edges, indicates that this increased rate of recovery might be related to proximity to seed sources and differences in substrates within the debris flow. Thus, factors other than type of disturbance might explain more of the variability in maximum rate of increase than in other variables.

Conclusions

Our approach demonstrated the advantages of using growth curves for change analysis. Inherent in the growth curves were all of the parameters relating to the trends in growth changes over time. The particular parameter of interest for a particular hypothesis can be extracted from the curve and returned to a GIS layer for spatial analysis. These parameters can be extracted by solving the curve for a particular level of the response variable (e.g., when did vegetation cover reach a certain level or when was maximum vegetation cover reached), a particular time (e.g., what was the estimated cover percentage at a particular year or what was the maximum cover reached), or other properties of the curve (integral, maximum first derivative, or order of the polynomial).

We believe that our approach will be most useful when the question of interest relates to pixel level trends, as opposed to categorical changes. For our study in disturbance recovery, this involved changes in green vegetation cover over time. In addition to disturbance ecology, other areas of study that we believe would benefit from this approach include (1) growth rates of forest stands, such as increases in biomass in managed forests, (2) successional processes, such as changes from deciduous forests to mixed stands to conifer, (3) seasonal changes associated with plant phenology, or (4) rates of urbanization, such as changes at the pixel level in percent of land converted from agriculture to urban, but not categorical changes in pixels from agricultural to urban. Thus, this technique is applicable to sets of continuous data (not thematic), with more than two dates, where the question of interest relates primarily to trends.

Acknowledgments

The authors wish to acknowledge the assistance of Warren Cohen, U.S. Forest Service Pacific Northwest Research Station, Doretta Collins, Washington State Department of Natural Resources, Thomas Erkert, Gifford Pinchot National Forest, and Peter Frenzen and Gordon Glockner, Mount St. Helens National Volcanic Monument, for their support in this project. Frederick Swanson, U.S. Forest Service Pacific Northwest Research Station, Janet Franklin, San Diego State University, and Peter Frenzen provided constructed reviews of a draft of this article. Partial funding for this project was provided through the National Science Foundation (grant #GER-9452810) under the auspices of the NSF Graduate Research Fellowship in Landscape Studies.

References

Armesto, J. J., and Pickett, S. T. A. (1986), Removal experiments to test mechanisms of plant succession in oldfields, *Vegetatio* 66:85-93.

Collins, J. B., and Woodcock, C. E. (1996), An assessment of several linear change detection techniques for mapping forest mortality using multitemporal Landsat TM Data, *Remote Sensing of Environment* 56:66-77.

Coppin, P. R., and Bauer, M. E. (1996), Digital change detection in forest ecosystems with remote sensing imagery, *Remote Sensing Reviews* 13:207-234.

del Moral, R., and Bliss, L. C. (1993), Mechanisms of primary succession: insights resulting from the eruption of Mount St. Helens, In *Advances in Ecological Research*, vol 24 (M. Began and A. Fitter, Eds.), Academic Press, London, pp. 1-66.

Eastman, J. R., and Fulk, M. (1993), Long sequence time series evaluation using standardized principal components, *Photogrammetric Engineering and Remote Sensing* 59:1307-1312.

Franklin, J. F., Frenzen, P. M., and Swanson, F. J. (1988), Re-creation of ecosystems at Mount St, Helens -- contrasts in artificial and natural approaches, In *Rehabilitating Damaged Ecosystems* (J. Cairns, Jr., Ed.), CRC Press, Boca Raton, Florida, pp. 1-37.

Franklin, J. F., MacMahon, J. A., Swanson, F. J., and Sedell, J. R. (1985), Ecosystem responses to the eruption of Mount St. Helens, *National Geographic Research* 1:198-216.

Frenzen, P. (1992), Mount St. Helens: a laboratory for research and education, *Journal of Forestry* 90:14-18,37.

Halpern, C. B., and Franklin, J. F. (1990), Physiognomic development of *Pseudotsuga* forests in relation to initial structure and disturbance intensity, *Journal of Vegetation Science* 1:475-482.

Halpern, C. B., Frenzen, P. M., Means, J. E., and Franklin, J. F. (1990), Plant succession in areas of scorched and blown-down forest after the 1980 eruption of Mount St. Helens, Washington, *Journal of Vegetation Science* 1:181-194.

Halpern, C. B., and Harmon, M. E. (1982), Early plant succession on the Muddy River mudflow, Mount St. Helens, Washington, *The American Naturalist* 110:97-106.

Heger, L. (1968), A method of constructing site-index curves from stem analyses, *The Forestry Chronicle* 21:11-15.

Hunt, R. (1982), *Plant Growth Curves: The Functional Approach to Plant Growth Analysis,* University Park Press, Baltimore. 248 p.

Lambin, E. F., and Strahler, A. H. (1994), Change vector analysis in multitemporal space: a tool to detect and categorize land-cover change processes using high temporal-resolution satellite data, *Remote Sensing of Environment* 48:231-244.

Lawrence, R. L., and Ripple, W. J. (in press), Comparisons Among Vegetation Indices and Bandwise Regression in a Highly Disturbed, Heterogeneous Landscape: Mount St. Helens, Washington, *Remote Sensing of Environment.*

Lillesand, T. M., and Kiefer, R. W. (1994), *Remote Sensing and Image Interpretation*, 3rd ed., John Wiley & Sons, Inc., New York. 750 p.

Lipman. P. W., and Mullineaux, D. R., Eds. (1981), *The Eruptions of Mount St, Helens, Washington,* Geological Survey Professional Paper 1250, U.S. Government Printing Office, Washington, D.C. 844 p.

MathSoft, Inc. (1995), *S-PLUS Users' Manual*, MathSoft, Inc., Seattle.

Means, J. E., McKee, W. A., Moir, W. H., and Franklin, J. F. (1982), Natural revegetation of the northeastern portion of the devastated area, In *Mount St. Helens -- Five Years Later* (S. A. C. Keller, Ed.), Eastern Washington University Press, Cheney, WA, pp. 93-103.

Muchoney, D. M., and Haack, B. N. (1994), Change detection for monitoring forest defoliation, *Photogrammetric Engineering and Remote Sensing* 60:1243-1251.

Olsson, H. (1994), Changes in satellite-measured reflectances caused by thinning cuttings in boreal forests, *Remote Sensing of Environment* 50:221-230.

Peterson, U. (1992), Seasonal reflectance factor dynamics in boreal forest clear-cut communities, *International Journal of Remote Sensing* 13:753-772.

Peterson, U., and Nilson, T. (1993), Successional reflectance trajectories in northern temperate forests, *International Journal of Remote Sensing* 14:609-613.

Reed, B. C., Brown, J. F., VanderZee, D., Loveland, T. R., Merchant, J. W., and Ohlen, D. O. (1994), Measuring phenological variability from satellite imagery, *Journal of Vegetation Science* 5:703-714.

Richards, F. J. (1959), A flexible growth function for empirical use, *Journal of Experimental Botany* 10:290-300.

Samson, S. A. (1993) Two indices to characterize temporal patterns in the spectral response of vegetation, *Photogrammetric Engineering and Remote Sensing* 59:511-517.

Chapter 4. Fifteen Years of Succession at Mount St. Helens: A Landscape Perspective

Rick L. Lawrence and William J. Ripple

Forest Resources Department,
Oregon State University,
Corvallis, Oregon,
January 14, 1998.

Abstract

We used satellite remote sensing and a geographic information system to examine the key factors controlling the revegetation of Mount St. Helens in the first 15 years following its catastrophic eruption in 1980. The study area consisted of only those portions of the Mount St. Helens devastated area that have been allowed to recover with a minimum of human management.

Eight Landsat satellite scenes from 1984 to 1995 were geometrically and radiometrically corrected to each other and transformed to estimated green vegetation cover for each scene. We fit growth curves to each pixel for the multitemporal data and, to represent response variables, extracted parameters of interest from the growth curves. These response variables included, for each pixel, (1) the number of years to reach an estimated 10% vegetation cover, (2) maximum rate of increase in vegetation cover, (3) time-integrated vegetation cover, and (4) maximum estimated cover reached during the study period. Explanatory variables included type of volcanic disturbance, topographic variables, distance from roads and streams, initial tephra thickness, and pre-eruptive conditions. Regression tree analysis was used to model the response variables with the explanatory variables.

Regression tree analysis explained 50% of the variation in years to reach 10% estimated cover, 57% of the variation in time-integrated estimated cover, 31% of the variation in maximum rate of estimated cover increase, and 51% of the variability in maximum estimated cover. Remaining variability was a function of other variables, stochastic factors, and image processing. The most important determinant of revegetation

was the presence or absence of biotic legacies, as evidenced by volcanic disturbance impacts. This stratified the study area into primary and secondary succession areas. Under secondary succession conditions, gradients of biotic legacies were evident. Factors affecting the establishment and growth of survivors were important, including original tephra thickness and erosional processes. In areas of primary succession, erosional processes were important in mitigating site conditions for colonizing seeds. Distance from seed sources was important primarily near forested edges. Additional topographic variables, including elevation, aspect, and slope curvature, had limited importance. We were not able to detect significant landscape-scale effects of streams, roads, or pre-eruption vegetation conditions.

Introduction

The volcanic eruption of Mount St. Helens in the State of Washington on May 18, 1980, provided an outstanding opportunity for scientific research (Frenzen, 1992). The proximity of Mount St. Helens to major population centers in the Pacific Northwest made the site available to a large number of scientists from a wide diversity of fields (Franklin et al., 1988). In 1982, Congress established the Mount St. Helens National Volcanic Monument, thereby ensuring that natural processes would be allowed to "proceed substantially unimpeded" over a large portion of the mountain's blast zone. This designation enables long-term studies of ecosystem recovery, like the study reported here.

The particular nature of this eruption of Mount St. Helens also contributes to the special opportunities for research at this site. This eruption involved several types of disturbance events, including (1) a large debris avalanche that covered the area between the crater and Spirit Lake, as well as 20 km down the Toutle River Valley to the west of the mountain, (2) a lateral blast of steam and rock in a 180° arc to the north of the crater, which carried away all vegetation near the crater, blew down trees farther from the crater over a 550 km^2 area, and scorched and killed vegetation at the edges of the blast zone with temperatures up to 350°C, (3) mudflow deposits resulting from a variety of processes, including melting of glaciers and snowfields on the east, south, and west sides of the mountain, (4) pumiceous pyroclastic flows up to 850°C, which continued for months after the initial eruption, and (5) a layer of airfall tephra extending primarily to the northeast of the mountain (Lipman and Mullineaux, 1981). These disturbances not only differed in physical processes, but, as a result, differed in the type of deposits left behind and potential for survival of underground vegetation or seeds. This variability allowed us to compare recovery from differing disturbance mechanisms side-by-side within a limited geographic area.

The pattern of these various disturbances resulting from the Mount St. Helens eruption also contributes to the opportunity to research landscape-scale recovery processes. The lateral blast was directed to the north of the crater, the debris avalanche traveled north and east, the mudflows spread east, south and west, the pyroclastic flows occurred primarily to the north, and the airfall tephra traveled primarily northeast. As a result, the patterns of disturbance are not highly correlated with factors such as elevation or distance from surviving seed sources. This lack of correlation facilitates statistical analyses of vegetation recovery patterns. The diversity of disturbance patterns at Mount St. Helens also provides special challenges for studies of recovery (Frenzen, 1992). As early as 1985, it was noted that this diversity, which in turn results in a diversity of recovery patterns, "makes apparent the inadequacies of simple models in characterizing or explaining successional patterns" (Franklin et al., 1985). Further, previous studies have found that stochastic factors have played a major role in the early recovery of Mount St. Helens and might in some cases dominate mechanisms that can be modeled (del Moral and Bliss, 1993). These chance events might mask ecological processes of interest.

The objective of our study was to conduct the first landscape-scale examination of the patterns and processes of the recovery at Mount St. Helens using satellite imagery and a geographic information system (GIS). More specifically, we were interested in determining whether patterns and processes that have been detected in fine-scale studies were important at landscape scales.

Hundreds of field studies have been published regarding the recovery of Mount St. Helens (Frenzen et al., 1994). However, it has been necessary for time to pass for landscape-scale patterns to be readily detectable. As a result, reported studies to date have been at finer than landscape scales. Based on our review of these previous studies, we developed several hypotheses regarding landscape-scale patterns that could be evaluated with the use of satellite remote sensing and a GIS:

Hypothesis #1: Patterns of vegetation recovery within the Mount St. Helens devastated area are significantly dependent on pre-eruption biotic legacies, including surviving seeds and roots, organic debris, and organic soils.

Hypothesis #2: Patterns of vegetation recovery within the Mount St. Helens devastated area are significantly correlated to topographic variables.

Hypothesis #3: Vegetation recovery within the Mount St. Helens devastated area is significantly positively correlated with proximity to streams.

Hypothesis #4: Vegetation recovery within the Mount St. Helens devastated area is significantly negatively correlated with proximity to roads.

Hypothesis #5: Vegetation recovery within the Mount St. Helens devastated area is significantly related to pre-eruption vegetation conditions.

Importance of Biotic Legacies

In large portions of the Mount St. Helens devastated area, biotic legacies persisted after the eruptions. These legacies included surviving seeds and roots, accessible organic soils, and organic debris, most notably downed trees. Studies in disturbance ecology have examined the relative importance for revegetation of post-disturbance sites of colonizing plants versus survivors (*e.g.*, Halpern and Franklin, 1990). Traditional theories of succession argue for the importance of colonizing species (Egler, 1954). According to these theories, following disturbance certain species well adapted to early successional conditions, such as nitrogen fixers and sun tolerant species, will colonize a site (Connell and Slatyer, 1977). These species are expected to facilitate later successional species, for example, by fixing nitrogen or providing protective shade. Such mechanisms can provide for a predictable successional sequence. Predictable successional patterns have been postulated specifically for post-eruption volcanic sites (e.g., Smathers and Mueller-Dombois, 1974).

An alternate theory of succession argues that stochastic elements are of greater importance than species characteristics and interactions in determining successional pathways (Vitousek and Walker, 1987). Thus, although certain species may be better adapted for success on early successional sites, site histories, including plants or seeds surviving disturbance, can be more important than colonizing species in determining site species composition.

Mount St. Helens has provided an opportunity to compare the relative importance of colonizing versus surviving species on a landscape-scale disturbance. Early studies of post-eruption vegetation showed dominance by surviving individuals at some sites (Franklin et al., 1985). In some cases, these surviving plants had been protected by a heavy but patchy Spring snowpack (Frenzen, 1992). Several early studies of revegetation on Mount St. Helens reported revegetation mostly from survivors within the devastated area (Franklin et al., 1985), while others documented invasion from forested edges (Halpern and Harmon, 1982). At the scale of study plots, revegetation sources might depend primarily on post-eruption microsite conditions (del Moral and Wood, 1993; Halpern et al., 1990).

Numerous studies of Mount St. Helens have focused on the effects of site variables on revegetation. The eruption of Mount St. Helens created a complex mosaic of volcanic deposits, in large part depending on the nature of the volcanic process (Figure 8). Several studies have found that revegetation is related to the nature of the volcanic disturbance (del Moral and Bliss, 1993; Means et al., 1982). Both the composition of resulting

Figure 8. Study area map, showing major types of volcanic disturbance resulting from the 1980 eruptions of Mount St. Helens. See Table 9 for a more detailed description of the disturbance types and sub-categories. Map is based on Lipman and Mullineaux (1981).

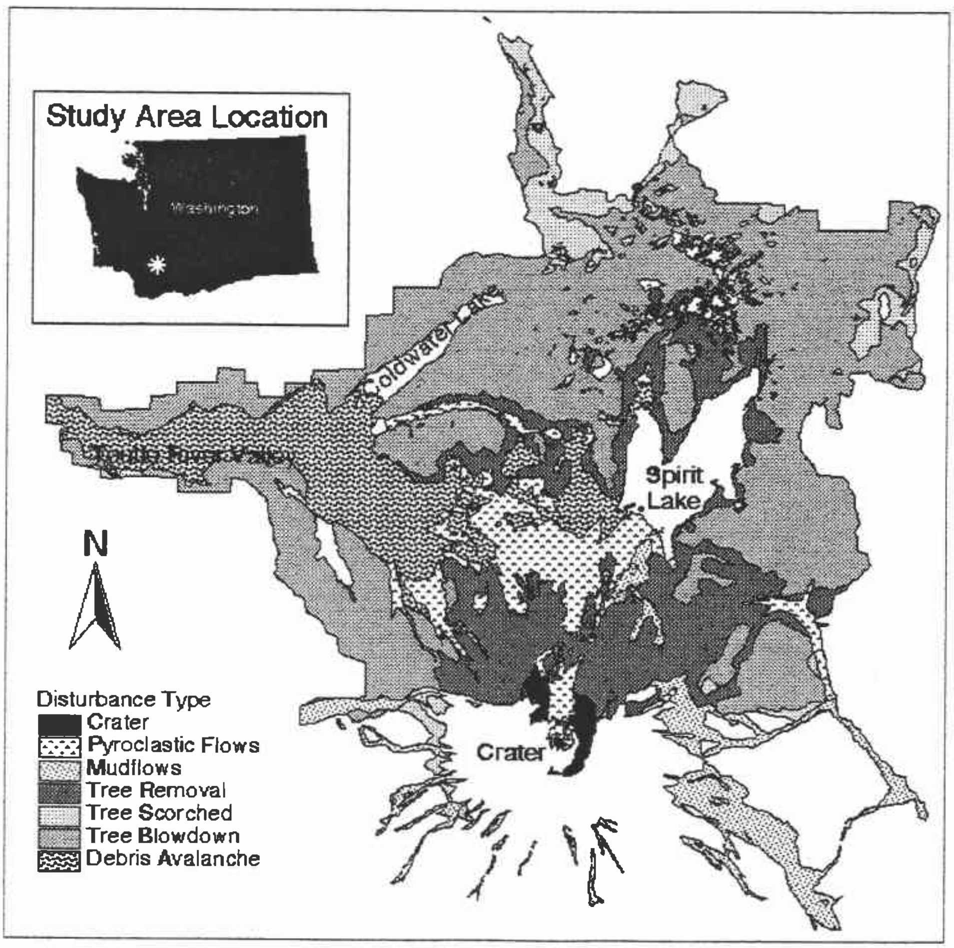

substrates and the presence of survivors are largely dependent on the disturbance type (Lipman and Mullineaux, 1981). Further, the thickness of airfall tephra from site to site partially governs the availability of acceptable substrates and, in turn, seedling success (Frenzen and Franklin, 1985; Halpern et al., 1990).

Importance of Topographic Variables

Topographic variables might be expected to significantly affect revegetation rates. In some cases, lower elevations are closer to colonizing seed sources. Topographic aspect is generally associated with differences in site quality. Steeper slopes might be expected to have greater erosion of tephra layers, resulting in thinner tephra layers (del Moral, 1983), while flat areas at the base of steep slopes might be expected to accumulate tephra. In addition, ridges might have protected some areas from the direct impact of the eruption. However, in a study comparing the effects of topographic variables to other variables in blown down and scorched forests, topographic variables were found not to be significantly correlated to rates of revegetation (Halpern et al., 1990).

Importance of Streams

The effect of streams within the devastated area has also been found to significantly affect revegetation (Halpern and Harmon, 1982). Within riparian areas, revegetation has been found to be more rapid away from streams because of the greater levels of scouring that takes place within active channels (Kiilsgaard et al., 1986). However, stream channels and gullies also have the effect of eroding tephra layers to uncover better seeding medium and providing water for growth (Antos and Zobel, 1987). Thus, revegetation might be greater near streams than elsewhere in the devastated area.

Importance of Roads

We believed that roads might have an effect on patterns of revegetation at the landscape scale, although this effect has not been studied previously at Mount St. Helens. Certainly, no revegetation can take place on roads. Road building activities might remove or bury surviving vegetation within the immediate vicinity of roads. Roadsides might support certain species because of the particular conditions present, such as additional disturbance and removal of shading. In addition, seeding along roads to prevent erosion might have both an effect in the immediate vicinity of the road and an effect that decreases with distance from roads.

Importance of Pre-Existing Vegetation Conditions

Although the eruption appeared to completely transform the Mount St. Helens landscape, vegetation conditions prior to the eruption might have an effect on post-eruption succession. Certainly, areas that were unvegetated prior to the eruption would generally not be expected to show significant revegetation in the years following the eruption. On the other hand, areas that were clearcut shortly before the eruption were found to recover more rapidly than forested areas, probably because of the presence of disturbance-adapted species on the clearcut sites (Means et al., 1982).

Study Area

The 1980 eruption of Mount St. Helens created a 550 km^2 devastated area in which substantially all above-ground vegetation was removed, buried, or otherwise killed. Although a portion of the devastated area was included in the Mount St. Helens National Volcanic Monument (the Monument), other portions were either owned privately or were outside the Monument boundary but within the Gifford Pinchot National Forest. We limited our study to natural processes and, as a result, only included in our study site the portion of the devastated area within the Monument boundary (Figure 8). The study area consisted of approximately 25,400 hectares, or approximately 46% of the area devastated by the eruption. Some of the specific characteristics of the study area are presented under Methods in our discussion of explanatory variables.

Vegetation structure and types are not readily summarized for the study area because plant cover is highly variable, within-site plant diversity is often high, and successional changes are, in some cases, rapid, making previous reports rapidly dated. Early reports of vegetation in blowndown forests reported 0.2% mean canopy cover in 1981, with dominant species primarily herbaceous, including pearly everlasting (*Anaphalis margaritacea)*, thistle (*Cirsium* spp.), fireweed (*Epilobium* spp.), ryegrass (*Lolium* spp.), and groundsel (*Senecio* spp.) (Franklin, et al., 1985). By 1992, these species had completely covered portions of the landscape (Frenzen, 1992). In subalpine study sites, substantially different patterns have been reported (del Moral and Bliss, 1993). Recovery has varied depending on the nature of the disturbance, with less than 1% cover reported on pyroclastic flows, under 5% on mudflows, and over 40% on adjacent tephra covered sites. Although there is significant overlap in species composition among these sites, dominance varies greatly. In 1990, the most abundant species on subalpine tephra sites included, in order of importance, bentgrass (*Agrostis diegoensis),* prairie lupine (*Lupinus lepidus*), spreading phlox (*Phlox diffusa*), and Newberry fleeceflower (*Polygonum newberryi*), and on a subalpine mudflow Newberry fleeceflower, prairie lupine, and Cardwell's penstemon (*Penstemon cardwellii*). However, there was significant change in the relative importance of species on the mudflow site between 1988 and 1990, emphasizing the rapid changes taking place within the area. Although tree species are not yet of significant influence within the Mount St. Helens devastated area, in some areas late snowpacks at the time of the eruption protected mountain hemlock (*Tsuga mertensiana*) and Pacific silver fir (*Abies amabilis*). Scattered alder (*Alnus* spp.) and Douglas-fir (*Pseudotsuga menziesii*) have appeared throughout the area, and some roots of willows (*Salix* spp.) and black cottonwood (*Populus trichocarpa*) that were up-rooted by mudflows and the debris avalanche happened to come to rest at the surface and resprout (Frenzen, 1992).

Methods

We used satellite images, a GIS, and statistical analyses to examine the relative importance of factors on landscape-scale revegetation of Mount St. Helens. Satellite imagery was used to characterize patterns of revegetation for the period 1980 to 1995. GIS layers were constructed to provide the explanatory data for our analysis.

Response Variables

Conceptually, our response variable was revegetation of the Mount St. Helens devastated area. However, characterization of revegetation is not simple. In one sense, revegetation can be characterized by the change in vegetation amount between two dates. For Mount St. Helens, where virtually no live, above-ground vegetation was present at the start of the study period, revegetation could then be calculated as the amount of live vegetation at the end of the study period. However, this analysis cannot differentiate among processes that might result in identical beginning and ending values, but follow

Figure 9. Two hypothetical growth curves showing increases in percent vegetation cover as a function of time. Both curves begin at 0% cover and end at 50% cover. Differences in curve shape indicate potential differences in processes influencing growth.

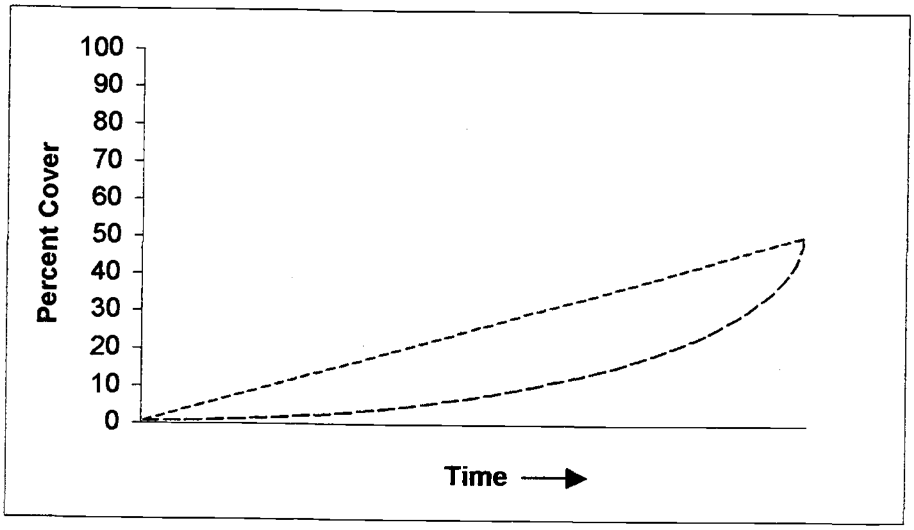

very different paths of growth. Figure 9 illustrates two different vegetation cover growth trajectories for two hypothetical plots. In both cases vegetation cover begins at 0% and rises to 50%. However, the differences in growth trajectories are a strong indication that key processes driving growth are operating differently for the two plots.

To differentiate among different growth trajectories, we utilized a method to characterize these trajectories from multitemporal satellite imagery. For this analysis, we acquired Landsat Thematic Mapper (TM) images for eight dates (19 July 1984; 26 August 1986; 31 August 1988; 9 September 1991; 10 August 1992; 29 August 1993; 31 July 1994; and 19 August 1995). All images were geometrically corrected to the 1991 scene and radiometrically corrected to the 1995 scene. Images were masked to the study area using a single mask. Finally, the images for each year were converted to estimated percent of green vegetation cover (Estimated Cover) based on a regression formula developed with the 1995 image (Lawrence and Ripple, in press). The formula, which was found to predict Estimated Cover better than vegetation indices, was based on the relationship between the 1995 image spectral response and percent green vegetation cover, as estimated from aerial photographs. The relevant formula was:

$$\text{Estimated Cover} = 106.00 - 5.50\, B_{RED} + 0.048\, B_{RED}^2 + 1.36\, B_{NIR} - 0.0051\, B_{NIR}^2$$

where: Estimated Cover = percent of pixel covered by green vegetation as estimated by spectral bands

B_{RED} = red band (Landsat TM band 3; 0.63-0.69 μm) digital value

B_{NIR} = near infrared band (Landsat TM band 4; 0.76-0.90 μm) digital value

Growth curves were fit to nine dates of data (eight dates from the satellite images, plus we assumed no green vegetation cover immediately following the eruption) using a two step process. First, the nine dates of data were clustered into 24 classes having similar growth trajectories using a non-hierarchical, iterative, clustering algorithm. We then fit polynomial growth curves to the mean values of the 24 classes. From these fitted growth curves, we were able to extract parameters of interest representing different measures of revegetation.

We wanted to be able to compare early vegetation responses with longer-term responses and overall responses. Therefore, we selected response parameters that measured these different types of responses. To measure early vegetation responses, we compared how long different sites took to reach a threshold level of revegetation. For each pixel within our study image, we used the growth curves to calculate the number of years that were necessary to reach 10% Estimated Cover (Years to 10% Cover). We selected the 10% level because it was the minimum amount of vegetation distinction that was used to calculate Estimated Cover from aerial photographs. Thus, this was the minimum level of vegetation response in which we had confidence in estimating.

Selection of a single year to measure revegetation late in the study period might over or under estimate the response depending on the phenologic and other characteristics of a given site and year. Therefore, we selected the highest Estimated Cover (Maximum Estimated Cover) during the study period as our late response variable. Maximum Estimated Cover was estimated by finding the maximum value for each growth curve. To characterize overall vegetation response, we used two variables: (1) a measure of overall magnitude of the curve, as determined from the total area under the growth curve, or integral, during the study period (Time-Integrated Cover), and (2) a characteristic of the shape of the curve, based on the maximum rate of increase in the growth curve, or maximum first derivative, during the study period (Maximum Rate).

Explanatory Variables

Extensive fine-scale research has been conducted at Mount St. Helens regarding various factors affecting vegetation recovery, and our hypotheses were based on these studies. We selected explanatory variables that would enable us to test these hypotheses at the landscape scale.

Biotic Legacies. The presence, abundance, and success of survivors, as well as the availability of organic soils and the presence of organic debris, are a function of initial disturbance processes, varying degrees of disturbance intensity within these processes, and subsequent geomorphic processes. The importance of colonizers can be related to distance from colonizing seed sources.

Table 9. Types and intensity of disturbances resulting from the eruption of Mount St. Helens, based on classification by U.S. Geological Survey (Lipman and Mullineaux, 1981).

TYPE	THICKNESS	TEMPERATURE	SPEED
Pumiceous pyroclastic flow deposits			
Deposits of October 16-18	≤ 40 m	300°-700° C	≤ 100 km/hr
Deposits of August 7			
Deposits of July 22			
Deposits of June 12			
Deposits of May 25			
Deposits of May 18			
Mudflow features			
Mudflow deposits	≤ 4 m	< 100° C	4-110 km/hr
Mudflow-scoured areas	0		
Features of the directed blast			
Blast pyroclastic flow	≤ 10 m	70°-277° C	100-600 km/hr
Blast deposit above treeline	≤ 1 m	100°-350° C	
Scorched zone			
Tree-down zone			
Tree-removal zone			
Debris-avalanche deposits			
Mudflow unit	20-195 m	68°-98° C	140-220 km/hr
North Toutle unit			
Spirit Lake unit			
Coldwater Ridge unit			
Marginal unit			

To compare the effects of different disturbances resulting from the volcanic eruption, we manually digitized a map of disturbance types prepared by the U.S. Geological Survey (Lipman and Mullineaux, 1981). The resulting GIS layer was georeferenced to a Universal Transverse Mercator grid and converted to raster (grid-cell) format with 25 m pixels (as were all GIS layers). The original map classified 26 different disturbance types, 18 of which occurred in our study area (Table 9).

Our disturbance type layer accounted for much of the variation in intensity of volcanic disturbance, since intensity in terms of heat, impact force, and deposit thickness is related to disturbance type. However, within disturbance types, it was possible that areas farther from the eruption would generally receive less intense disturbance. We prepared a GIS layer showing distance from each point in the study area to the crater to test whether this variable was important in vegetation recovery. Distances extended up to 21.3 km. In addition, some areas were partially shielded by ridges and other topographical features from the direct impact of the lateral blast. The location of the highest point of the eruption's origin was estimated from published photographs of the eruption (Voight, 1981). We determined which areas were shielded from this point and prepared a binary GIS layer showing topographically-protected versus topographically-unprotected areas.

Post-eruptive geomorphic processes are largely a function of slope gradient and curvature. Using a 30 m digital elevation model as our base data, slope gradient was calculated in degrees from horizontal and ranged from 0° to 68°. As a measure of the erosional or depositional shape of the surface, the second derivative of the surface was calculated. Positive values reflected convex surfaces (potentially erosional) and negative values represented concave surfaces (potentially depositional).

To compare the effects of different thicknesses of airfall tephra within the devastated area, we manually digitized a map of tephra thickness prepared by the U.S. Geological Survey (Waitt et al., 1981). The original isopach map was based on ground sampling and classified tephra thickness within the study area in the following increments: 200 cm, 100 cm, 50 cm, 20 cm, 10 cm, 5 cm, and 2 cm. This explanatory variable did not account for subsequent erosion and deposition of tephra by post-eruption geomorphic processes or for local variations in tephra thickness.

In order to test the importance of colonizers, it was necessary to determine whether distance from sources of colonizing seed was an important determinant for revegetation. We computed the distance from each point in the study area to the nearest point classified on the disturbance layer as forested and affected only by the deposition of airfall tephra. Distances from seed sources within the study area ranged from 25 m to 8225 m.

Topographic variables. Although topographic variables have not been found significant in previous studies of revegetation at Mount St. Helens, we believed that they might be important at the landscape scale. Vegetation gradients commonly occur across topographic gradients. Using a 30 m digital elevation model as our base data, we created several GIS layers (in addition to slope gradient and curvature) to test the effects of topography. The digital elevation model was used in its original form to provide elevation data in meters above sea level. Elevation within the study area ranged from 476 m to 2493 m. Aspect was calculated into five classes, north, east, south, west, and flat.

Streams. To test the impact of streams on vegetation recovery at the landscape scale, we prepared two GIS layers. The first layer was binary, showing areas as either within a 25 m wide riparian zone centered on a stream (our finest level of resolution) or outside the zone. To test whether there was a broader effect of streams, we also prepared a layer showing the distance from each point in the study area to the nearest stream.

Roads. Although previous studies have not looked at the impact of roads on revegetation within the devastated area, we have observed an apparent effect that was visible in aerial photographs and on satellite images, although there are only three major roads within the study area. To test whether this effect was important at the landscape scale, we prepared two GIS layers. The first layer was binary, showing areas as either within a 25 m zone centered on a road or outside the zone. To test whether there was a broader effect of roads, we also prepared a layer showing the distance from each point in the study area to the nearest road.

Pre-Existing Vegetation Conditions. To test the importance of preexisting vegetative conditions, we classified a 1977 Landsat MSS image into three vegetation types, forested (consisting of 15,823 ha), meadow/recent clearcut (consisting of 5,653 ha), and unvegetated (consisting of 2,402 ha).

Statistical Analysis

We used regression tree analysis (RTA) to model our four response variables using our array of 14 explanatory variables. RTA is a relatively new, computationally intensive analytical approach (Efron and Tibshirani, 1991; Breiman et al., 1984). It operates by analyzing all explanatory variables and determining which binary division of a single explanatory variable best reduces deviance (defined as squared residuals) in the response variable. For each portion of the data resulting from this first split, the process is repeated. The splitting of data continues until homogeneous ending points (terminal nodes) are reached. The result is a hierarchical tree apportioning all of the data through a series of binary divisions. RTA generally will over-fit the model. Therefore, a method is then used to reduce or prune the tree to a level believed to be not over-fit.

RTA has advantages and disadvantages when compared to more traditional methods, such as multiple linear regression. Multiple linear regression applies explanatory variables continuously, rather than by binary splits, and is able to model the response variable continuously as well. This makes multiple linear regression an excellent tool when the relationship between the response variable and the explanatory variables is linear (or can be made linear through transformations) (Breiman et al., 1984). On the other hand, multiple linear regression does not readily handle non-linear relations and has difficulty modeling complex interactions, especially among continuous and categorical explanatory variables.

By comparison, because RTA operates on binary splits, linearity is not a consideration and, by the way the tree is structured, complex interactions can be readily modeled. Also, because RTA results in a limited number of terminal nodes that are the result of an equal number of paths through the tree, the results of RTA can be returned to a GIS for spatial analysis and display.

The choice of RTA versus other models, such as multiple linear regression, is largely governed by the relationships within the data. However, with a complex set of explanatory variables, the nature of the relationship can be difficult to determine. Because both multiple linear regression and RTA are based on minimizing squared residual deviance, the amount of variation explained by models (R^2 = (total sum of squares - residual sum of squares) / total sum of squares) can be directly compared between multiple linear regression and RTA models. Using the data from our analysis discussed below, we compared our RTA models with our best multiple linear regression fits using an independent validation data set of 1000 points. In all cases, RTA explained substantially more variability in the response variable than multiple linear regression. Therefore, we used RTA for our analysis.

We fit regression trees using RTA as implemented in the S-Plus statistical package (MathSoft, Inc., 1995; Venables and Ripley, 1994). For each of 5000 random points, we extracted all four response and all 14 explanatory variables. These data were transferred to an S-Plus data frame and regression trees were fit for each response variable.

To prune the regression trees, we used a cross validation method. This method began by randomly dividing the data into ten equal data sets, in our case of 500 points each. Trees were generated for nine of the data sets and validated against the tenth. The point of lowest mean square error for the validation is presumably the best size tree. However, different random divisions of the original data can produce different size trees. Therefore, we ran the cross validation procedure ten times and selected as the best tree size the smallest tree within one standard error of the mean of the ten runs. The original tree generated by the full data set was then pruned to the number of terminal nodes determined from the cross validations. This procedure was followed for each of the four response variables.

To further test the quality of the final regression trees, we validated the trees against an independent data set. We extracted response and explanatory variable data for a second random set of 5000 points. For this validation data, predicted values were produced from each final regression tree. These predicted values were used to calculate residual errors and coefficients of determination (R^2) for comparison with the original data sets used to produce the trees.

The final validated regression trees were used to prepare for each explanatory variable a GIS layer of predicted values. These GIS layers were used to analyze spatially the results of the regression trees.

Results

RTA resulted in four regression trees. The terminal nodes of the regression trees represented sets of predicted Estimated Cover values, each based on a unique path through the regression tree. The regression trees for Maximum Rate and Time-Integrated Cover were essentially identical except for the amount of variability explained. Because these response variables were both designed to measure overall response and because the tree for Time-Integrated Cover explained 19% more variability, we have presented the regression trees and related GIS layers only for Years to 10% Cover, Time-Integrated

Table 10. Amount of variability explained by each regression tree for 5,000 points used to model the regression trees and an independent set of 5,000 points.

Response Variable	R^2	Validation R^2
Years to 10% Cover	0.50	0.46
Time-Integrated Cover	0.57	0.54
Maximum Rate	0.37	0.31
Maximum Estimated Cover	0.51	0.47

Cover, and Maximum Estimated Cover (Figures 10, 11, and 12). For the validation data, these three regression trees explained within 4% of the variability explained in the original data (Table 10).

The regression trees can be used to determine the importance of each explanatory variable relative to each response variable, the conditions under which each explanatory variable is important, the predicted value for each path through the regression trees, and the total area for each predicted value. The spatial location for each path through the regression tree is mapped in the related GIS layers. For example, in the regression tree for Years to 10% Cover (Figure 10), for areas of secondary succession closer than 11 km to the crater and at slope gradients less than 15.5°, the predicted value is 19 years to reach 10% cover and 1,791 ha fit these conditions. Areas meeting these conditions are mapped in red together with areas having slope gradients greater than or equal to 15.5°, but otherwise meeting the same conditions. The presence and importance of each explanatory variable differed for each regression tree.

Figure 10. For Years to Reach 10% Cover, final regression tree and related GIS layer. Text at splits in the regression tree indicates conditions for the left branchings in the tree. Top numbers at ends of the tree are estimated years to reach 10% cover for observations meeting the conditions leading through the tree and bottom numbers are hectares meeting such conditions. Colored text in the tree is the key to colors in the GIS layer.

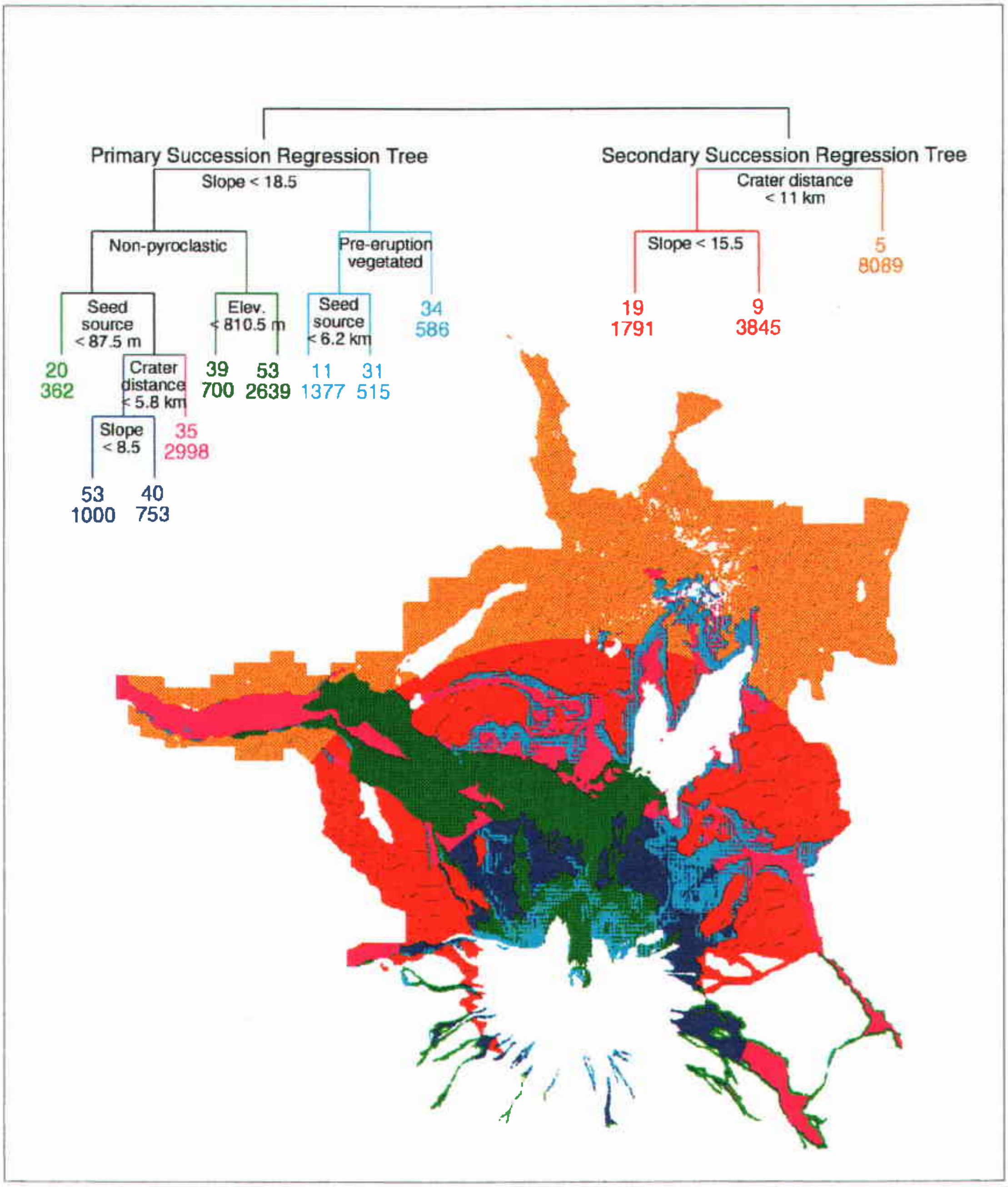

Figure 11. For Time-Integrated Cover, final regression tree and related GIS layer. Text at splits in the regression tree indicates conditions for the left branchings in the tree. Top numbers at ends of the tree are estimated time-integrated cover for observations meeting the conditions leading through the tree and bottom numbers are hectares meeting such conditions. Colored text in the tree is the key to colors in the GIS layer.

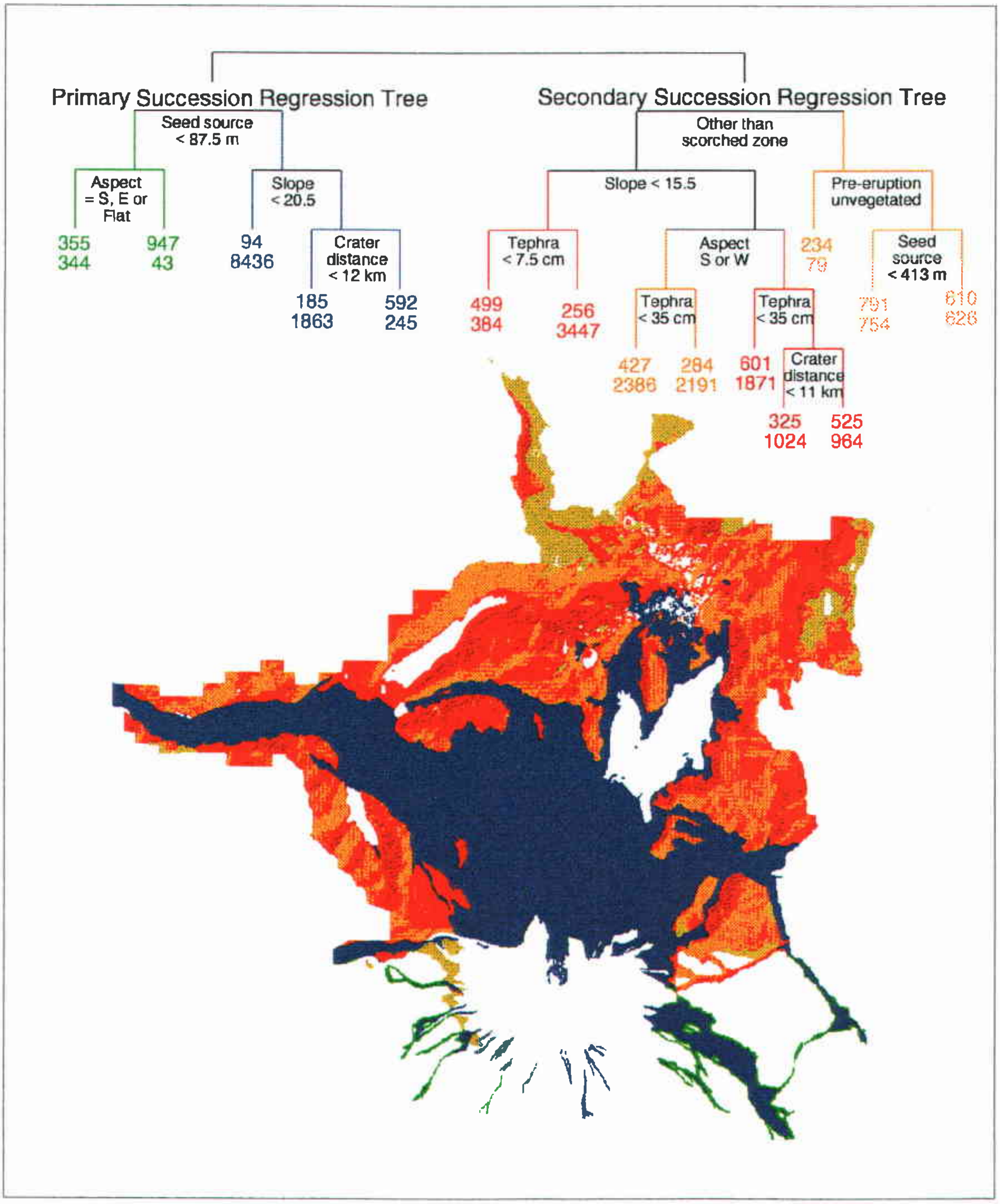

Figure 12. For Maximum Estimated Cover, final regression tree and related GIS layer. Text at splits in the regression tree indicates conditions for the left branchings in the tree. Top numbers at ends of the tree are estimated maximum cover for observations meeting the conditions leading through the tree and bottom numbers are hectares meeting such conditions. Colored text in the tree is the key to colors in the GIS layer.

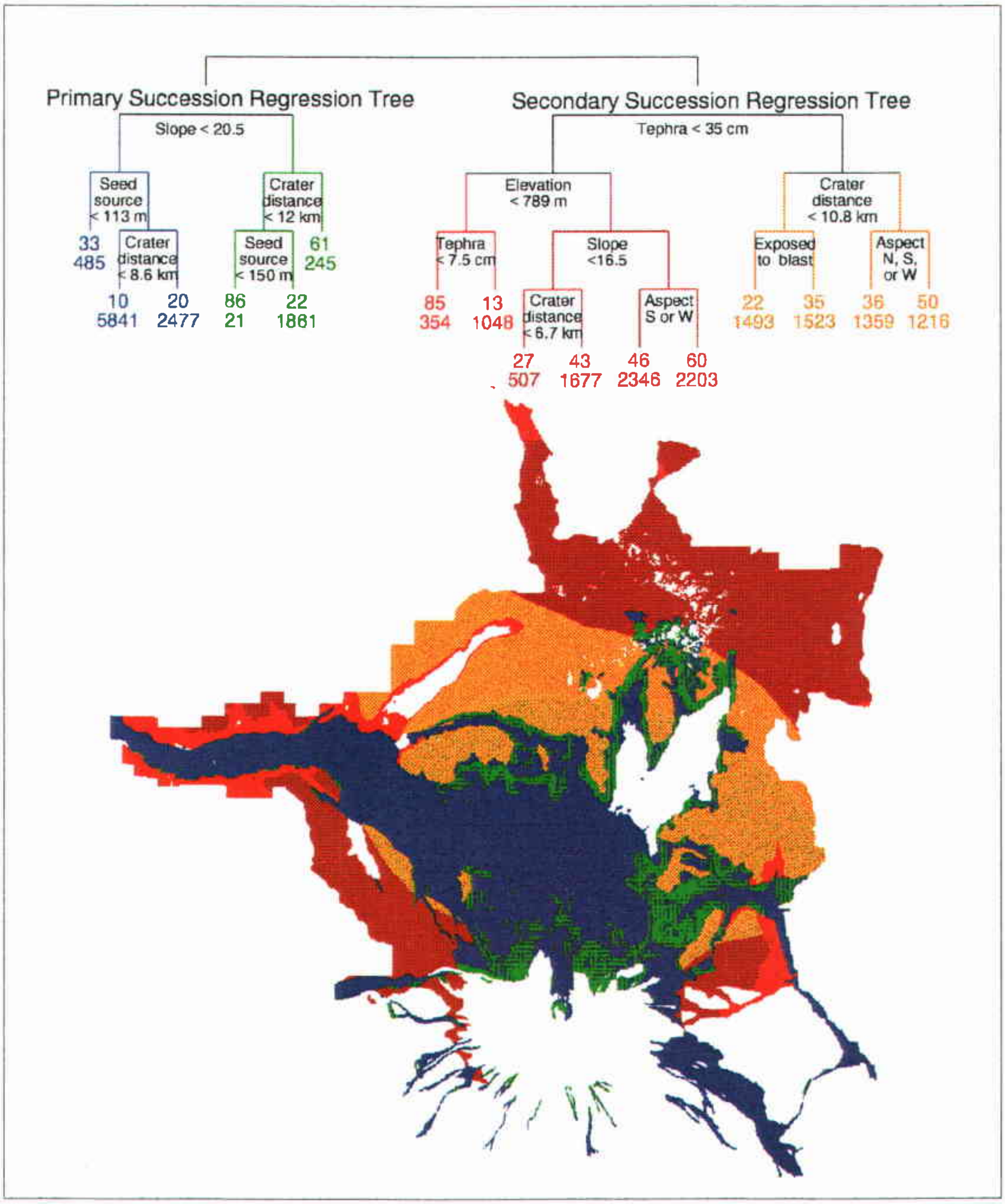

Disturbance Types. For all four regression trees, the first tree division was based on disturbance types. Observations from four disturbance types were directed to one side of the regression tree, while the remaining disturbance types were directed to the other side. These four disturbance types included the tree blowdown zone, the tree scorched zone, the mudflow-scoured areas, and the debris avalanche marginal unit. Disturbance types that were not included in this group included all pyroclastic flows, the main portions of the mudflows, the main portions of the debris avalanche, and the tree removal zone. Pyroclastic flows and most of the mudflows and debris avalanche were covered with thick deposits of juvenile soils and had essentially no surviving plant or sproutable plant parts (del Moral, 1983; del Moral and Bliss, 1993). The tree removal zone was an area of erosion caused by the lateral blast, which removed essentially all organic material from the zone. On the other hand, substantial amounts of surviving underground vegetation were found in the tree blowdown and tree scorched zones. The debris avalanche marginal unit consisted primarily of stream valley floor alluvium, which was rich in organic soils and debris. The mudflow scour areas were not subject to the thick residual deposits of the primary mudflows. Therefore, the first regression tree split effectively stratified the study area into (1) areas where survivors might be present or organic soils were thinly overlaid with volcanic deposits and (2) areas where biota and organic soils were either deeply buried, removed by erosion, or seared by heat. Although there might be a gradient of biotic legacies at Mount St. Helens, this initial division of the data for all response variables effectively stratified the study area into two portions: (1) areas without biotic legacies where primary succession is taking place and (2) areas with biotic legacies that are undergoing secondary succession.

Distance from Crater. Distance from the crater was important in all of the regression trees in areas of primary and secondary succession. For early vegetation response, this was important for all areas of secondary succession, but only for limited areas of primary succession. For Time-Integrated Cover and Maximum Estimated Cover on primary succession areas, distance from the crater was important only in limited areas of steeper slopes.

Shielding from Direct Impact. Whether an area was exposed or shielded from the direct impact of the lateral blast was generally not an important variable. The only exception was for Maximum Estimated Cover in areas of secondary succession close to the crater. The importance of this factor might be reflected in the type of disturbance, making this variable largely redundant.

Slope Gradient. Slope gradient was one of the most important explanatory variables, appearing in primary and secondary succession on all of the regression trees. Generally, slope gradient divided at about 15° to 20°, with greater recovery on steeper slopes. Areas where slope gradient was not important included, (1) for Years to 10% Cover, areas of secondary succession greater than 11 km from the crater, (2) for Time-Integrated Cover, areas at the edges of mudflows and tree scorched areas, and (3) for Maximum Estimated Cover, areas of secondary succession with airfall tephra greater then 35 cm and, for areas with thinner airfall tephra layers, areas lower than 789 m in elevation.

Slope Curvature. Slope curvature was not important in any of the regression trees.

Airfall Tephra Thickness. Initial thickness of airfall tephra was not important for early vegetation response. However, for Time-Integrated Cover and Maximum Estimated

Cover, original thickness of airfall tephra was important for almost all areas. Generally, the regression trees divided areas based on a tephra thickness of 35 cm, although in some areas a division based on 7.5 cm of tephra was important.

Distance from Colonizing Seed Sources. Distance from colonizing seed sources was important for primary succession for all of the regression trees. In most cases, this was observed at the edges of mudflows. For secondary succession, distance from colonizing seed sources was important only for Time-Integrated Cover in tree scorched areas.

Elevation. Elevation was one of the less important variables included in the regression trees. For early vegetation response, elevation distinguished a 700 ha area as the debris avalanche entered the Toutle River Valley. For Maximum Estimated Cover, elevation was important for secondary succession areas with less than 35 cm of airfall tephra.

Topographic Aspect. Aspect was not included in the regression tree for Years to 10% Cover, but was a component for the other regression trees. For Time-Integrated Cover, aspect was a factor at the edges of mudflows and on steep slopes where secondary succession was taking place. For Maximum Estimated Cover, aspect was important only in limited areas of secondary succession.

Streams. Neither the 25 m stream buffers nor general proximity to streams were included in any of the regression trees.

Roads. Neither the 25 m road buffers nor general proximity to roads were included in any of the regression trees.

Pre-Existing Vegetation Conditions. Pre-existing vegetation conditions were a factor in the regression trees for Years to 10% Cover and Time-Integrated Cover. However, the only distinctions made were whether areas were unvegetated prior to the eruption. This indicates a distinction for areas such as rock outcroppings, but not among vegetative conditions. This lack of distinction might be a function of our not distinguishing between meadows and clearcuts.

Discussion

Importance of Biotic Legacies

Our research strongly supported previous fine-scale findings regarding the importance of biotic legacies for revegetation following disturbance. Areas with biotic legacies can reflect gradients in the abundance of survivors. However, the initial stratification of the data for all response variables reflected the importance of distinguishing primary successional processes, where virtually no survivors were present (Vitousek and Walker, 1987). Primary succession requires colonization and involves the slow process of soil building and nitrogen accumulation, which can take centuries. In primary succession, both the limitation of available propagules and lack of mineralized nitrogen combine to create a slow process of plant establishment and growth.

By contrast, secondary succession is marked by an increase in available nutrients after a disturbance. Lack of competition as a result of removal of preexisting vegetation initially increases availability of all nutrients. Presence of survivors, either in the form of sprouting rootstock or seeds stored in the organic soils, provides conditions for potentially rapid growth.

Both primary and secondary successional processes have been studied at Mount St. Helens. Studies of recovery on subalpine plots have noted the very slow recovery on pyroclastic, mudflow, and debris avalanche zones (del Moral and Bliss, 1993). Soil building processes and their importance for vegetation growth in the primary successional areas of Mount St. Helens have been documented (Ugolini et al., 1991). Similarly, the importance of survivors in the early, rapid recovery of portions of Mount St. Helens also has been a well documented phenomena (Franklin et al., 1988). By definition, this is a process that can only occur under secondary succession conditions.

Although the slow pace of primary succession relative to secondary succession has been cited by previous authors, opportunities are rare to quantify the difference without substantial confounding factors. However, the presence of primary and secondary succession side by side at Mount St. Helens allowed us to make this comparison, while controlling for many factors. The regression trees quantified this difference in rates of succession. The average time to reach 10% Estimated Cover under primary succession was 38 years compared to eight years for secondary succession, almost five times as long. Average Maximum Estimated Cover during the study period for primary successional areas was 16%, compared to 44% for areas of secondary succession. Finally, for Time-Integrated Cover, areas of secondary succession averaged more than three times that of primary successional areas.

The importance of airfall tephra was also related to the presence of biotic legacies. Tephra thickness was not an important variable in areas of primary succession because the tephra simply added to the depth of juvenile soils. However, tephra thickness was an important factor for secondary succession both for Time-Integrated Cover and Maximum

Estimated Cover. This indicated that tephra thickness was important because it buried surviving vegetation, and the ability of vegetation to establish was related to the ability to penetrate tephra layers (Zobel and Antos, 1997).

Our results indicated that, within areas of secondary succession, gradients of biotic legacies probably exist. Within these areas, which were affected primarily by the lateral blast and airfall tephra, distance from the crater was an important factor, especially with respect to early vegetation response. This reflects a reduction in the heat and force of the lateral blast with distance from the crater, generally resulting in a greater abundance of survivors at greater distance.

The importance of surviving vegetation is also evidenced by the influence of post-eruption geomorphic processes. In areas of secondary succession, slope gradient was one of the most important factors, with slopes greater than 15° to 16° reaching 10% Estimated Cover faster, having greater Time-Integrated Cover, and achieving higher Maximum Estimated Cover. We believe that the erosional nature of steep slopes might have three functions leading to faster recovery in secondary succession: (1) erosion on steep slopes can reduce the thickness of volcanic layers, thereby enhancing the resprouting of surviving rootstocks; (2) erosion on steep slopes can uncover organic soils or reduce the volcanic layers covering organic soils, thereby enhancing seedling growth; and (3) erosion on steep slopes breaks the crust covering volcanic deposits and thereby enhances seedling establishment. The importance of slope gradient for recovery of surviving vegetation is supported by research at other volcanoes. A review of research at Katmai, Mexico, St. Vincent, the Philippines, and New Guinea revealed that erosion is key to the establishment and success of survivors (Antos and Zobel, 1987).

The importance of survivors relative to colonizers in secondary succession was supported by the lack of importance of distance from seed sources. Distance from seed sources was important only for Time-Integrated Cover within the tree scorched zone, where areas within 412.5 m of seed sources had 1.3 times the Time-Integrated Cover of areas farther than seed sources. Although it is unclear to us why this occurred, the presence of greater amounts of upright, dead vegetation in the scorched zone might capture wind blown seeds and result in a gradient of increased vegetation near seed sources.

Because primary succession is dependent on colonizing seed, seed source distance was also important for all response variables within these areas. However, the regression tree splits for seed distance were between 87 m and 150 m. Areas within this distance had greater recovery for all response variables. This phenomenon occurred only on mudflows to the east and south of the crater.

Our finding on seed source distance is consistent with an early study on the Muddy River mudflow to the east of the crater (Halpern and Harmon, 1982) and early studies of the Kautz Creek mudflow on nearby Mount Rainier (Frenzen et al., 1988). Seedling densities at each location dropped significantly in plots more than 100 m to 150 m from forested edges. This finding might be explained by a predominance of heavy, poorly dispersing seeds from the adjoining forests (Wood and del Moral, 1987). Thus, these seeds will have an impact primarily within short distances of seed sources. This result might also be related to the dynamics of the mudflows, which had less force and thinner deposits toward their edges. The absence of other, farther distance divisions indicates that distance from seed sources was probably not an important factor for light, wind blown seeds, which were the primary colonizers on primary succession sites at Mount St. Helens (del Moral and Bliss, 1993).

Importance of Topographic Variables

Of the various topographic variables (elevation, slope gradient, slope curvature, and aspect), slope gradient was the most important, while slope curvature was not included in any of the regression trees. We have already discussed the importance of slope gradient relative to survivors in secondary succession conditions. However, slope gradient was also very important for primary succession. In these areas, slopes steeper than 18° to 20° reached 10% Estimated Cover sooner, had greater Maximum Estimated Cover, and experienced greater Time-Integrated Cover. The exception was Time-Integrated Cover for 387 ha at the forested edges of mudflows. The nearly universal importance of this variable pointed to the impact of post-eruptive erosional forces at Mount St. Helens.

The importance of slope gradient on vegetation recovery has been documented at finer scales, although not previously quantified. It has generally been noted that erosion favors, while deposition hinders, recovery, and that this effect might be the most important post-eruptive factor for recovery (Franklin et al., 1988). The Soil Conservation Service, in its study of grass seeding at Mount St. Helens, noted greater success on steep slopes (Franklin et al., 1988). Although one plot-based study found tephra thickness sometimes significant, but not slope gradient (Halpern et al., 1990), that study measured tephra thickness at the time of the study, not initial thicknesses. Thus, erosion and deposition might already have taken place and was accounted for in the measurements. In contrast, our study used initial average tephra thicknesses as an explanatory variable.

These previous studies emphasized the importance of slope gradient on secondary succession, which we have discussed. However, we do not believe that the importance of slope gradient for primary succession has been well documented prior to this study.

Plot-based studies indicate the mechanisms favoring vegetation on steeper slopes. These studies have demonstrated the difficulty for germinating seeds in breaking through crusts at the surface of volcanic deposits and the resulting negative impact on seedling establishment (Frenzen and Franklin, 1985). Water erosion on slopes beyond a level of steepness can break this crust and help seedling establishment. Further, rills and gullies, which are more likely to form on steeper slopes, provide relatively safe areas for seedling germination and establishment (del Moral and Bliss, 1993).

Elevation was generally not important, except with respect to Maximum Estimated Cover on areas of secondary succession. This might indicate that surviving species and early successional species in this study area are not sensitive to the range of elevations present. However, species having greater importance toward the end of the study period might be more sensitive to elevation. Resolution of this issue will require additional fine-scale studies that are able to differentiate species.

The relative lack of importance for topographic aspect might be partially a function of the lateral blast. Because the blast was directed to the north of the crater, aspect is somewhat accounted for by disturbance type. However, aspect was important in limited circumstances.

Importance of Streams and Roads

Neither streams nor roads were included in any of the regression trees. Several factors might explain these results. First, our level of resolution was 25 m. If the primary effects of streams or roads are at a finer scale than 25 m, the effects might not be sufficient to significantly affect pixel values. Thus, the result might be an artifact of the scale of our study. Second, RTA analyzes data based on reducing residual variance. The effects of streams and roads might be present, but, on a landscape scale, might not be a major source of variation either because the areas affected by these features comprise a small percentage of the total landscape or because the degree of the effect is not large.

Importance of Pre-Existing Vegetation Conditions

We were not able to detect the effects of pre-existing vegetation conditions, other than areas that were not vegetated prior to the eruption. Again, several factors might explain this result. First, our approach did not distinguish between meadows and recent clearcuts. However, the hypothesized effect was a function of the presence of early successional species in clearcuts that would not dominate meadows. Thus, the combining of these two cover types might have masked a real effect. Second, the effect was reported only in very early studies of recovery at Mount St. Helens. The effect might have been transitory, and therefore not detected in our study.

Variability Explained

The final regression trees explained 50% of the variability in Years to 10% Cover, 51% of the variability in Maximum Estimated Cover, and 57% of the variability in Time-Integrated Cover. In each case, this left approximately half of the variability unexplained by our analysis. In each case, variability explained in the validation data was within 4% of the original data, indicating that the regression trees were very robust within our study area.

Although we would have liked the regression trees to explain more variability in the data, there were numerous factors that prevented higher levels. These factors can be categorized as (1) data quality driven, and (2) biogeologically driven. Several factors related to our sources of data resulted in variability that could not be explained by our explanatory variables. These factors included our estimation of vegetation cover (the regression formula used to convert satellite spectral bands to Estimated Cover explained 75% of the variation in vegetation cover estimated from aerial photographs), unquantified errors in radiometric and geometric normalizations performed to compare year-to-year satellite images, unquantified errors in GIS layers used to compute explanatory variables, and lack of perfect fit in fitting growth curves to multitemporal data.

Perhaps equally important were variances in vegetation recovery not modeled by our explanatory variables. For example, recent research at other study sites has established the importance generally of stochastic factors in successional processes (Halpern and Franklin, 1990; Vitousek and Walker, 1987). Previous studies of Mount St. Helens have found unexpectedly large amounts of variability in vegetation recovery attributable to stochastic factors (del Moral and Bliss, 1993; Franklin et al., 1985). Because of lack of data, we were not able to model, for example, the effects of wind patterns during the study period, localized differences in precipitation, or variability in year-to-year seed production within the surviving forests surrounding the devastated area. Yet each of the factors has potentially large effects on recovery.

Conclusions

No simple model can fully explain the recovery of Mount St. Helens. However, based on our study of landscape-scale patterns of recovery, coupled with previous fine-scale studies, several important conclusions can be drawn:

(1) The presence or absence of a biotic legacy is the most important factor in determining spatial and temporal patterns of vegetation recovery. Thus, although survivors were reported as dominating early recovery (Franklin et al., 1985), the effects are still the most important 15 years after the eruption. We believe this distinction between primary and secondary succession will dominate spatial recovery patterns at Mount St. Helens for many years. Mount St. Helens has provided us with a rare opportunity to quantify the differences in rates of primary and secondary succession.

(2) Where a biotic legacy exists, disturbance processes that create gradients of biotic legacies are important. Post-eruption events, especially erosion, are important for their effects on survivor establishment and growth.

(3) Topographic variables are important on a landscape scale in the recovery of vegetation at Mount St. Helens. Although slope gradient was the most important of these variables, elevation and aspect were important under limited circumstances.

(4) For primary succession, factors that relate to seed dispersal, seedling establishment, and plant growth are most important. The most important of these factors are erosion and distance to seed sources. Erosion, represented by slope gradient, is important not only for secondary

succession, as has been previously documented, but for primary succession as well.

Acknowledgments

The authors wish to acknowledge the assistance of Warren Cohen, U.S. Forest Service Pacific Northwest Research Station, Doretta Collins, Washington State Department of Natural Resources, Thomas Erkert, Gifford Pinchot National Forest, and Peter Frenzen and Gordon Glockner, Mount St. Helens National Volcanic Monument, for their support in this project. Frederick Swanson, U.S. Forest Service Pacific Northwest Research Station, Jerry Franklin, University of Washington, and Peter Frenzen provided constructive reviews of a draft of this article. Partial funding for this project was provided through the National Science Foundation (grant #GER-9452810) under the auspices of the NSF Graduate Research Fellowship in Landscape Studies.

References

Antos, J. A., and Zobel, D. B. (1987), How plants survive burial: a review and initial responses to tephra from Mount St. Helens, In *Mount St. Helens 1980, Botanical Consequences of the Explosive Eruptions* (D. E. Bilderback, Ed.), University of California Press, Berkeley. p. 246-261.

Breiman, L., Friedman, J. H., Olshen, R. A., and Stone, C. J. (1984), *Classification and Regression Trees*, Wadsworth International Group, Belmont, CA.

Connell, J. H., and Slatyer, R. O. (1977), Mechanisms of succession in natural communities and their role in community stability and organization, *American Naturalist* 111:1119-1144.

del Moral, R. (1983), Initial recovery of subalpine vegetation on Mount St. Helens, Washington, *American Midland Naturalist* 109:72-80.

del Moral, R., and Bliss, L. C. (1993), Mechanisms of primary succession: insights resulting from the eruption of Mount St. Helens, In *Advances in Ecological*

Research, vol 24 (M. Began and A. Fitter, Eds.), Academic Press, London, pp. 1-66.

del Moral, R., and Wood, D. M. (1993), Early primary succession on the volcano Mount St. Helens, *Journal of Vegetation Science* 4:223-234.

Efron, B., and Tibshirani, R. (1991), Statistical data analysis in the computer age, *Science* 253:390-395.

Egler, F. E. (1954), Vegetation science concepts. I. Initial floristic composition, a factor in old-field vegetation development, *Vegetatio* 4:412-417.

Franklin, J. F., Frenzen, P. M., and Swanson, F. J. (1988), Re-creation of ecosystems at Mount St. Helens -- contrasts in artificial and natural approaches, In *Rehabilitating Damaged Ecosystems* (J. Cairns, Jr., Ed.), CRC Press, Boca Raton, FL. p. 1-37.

Franklin, J. F., MacMahon, J. A., Swanson, F. J., and Sedell, J. R. (1985), Ecosystem responses to the eruption of Mount St. Helens, *National Geographic Research* 1:198-216.

Frenzen, P. M. (1992), Mount St. Helens -- a laboratory for research and education, *Journal of Forestry* 90:14-18, 37.

Frenzen, P. M., Delano, A. M., and Crisafulli, C. M., comps. (1994), *Mount St. Helens: Biological Responses Following the 1980 Eruptions -- An Indexed Bibliography and Research Abstracts (1980-93)*, Gen. Tech. Rep. PNW-GTR-342, Portland, OR: U.S. Department of Agriculture, Forest Service, Pacific Northwest Research Station, 149 p.

Frenzen, P. M., and Franklin, J. F. (1985), Establishment of conifers from seed on tephra deposited by the 1980 eruptions of Mount St. Helens, Washington, *American Midland Naturalist*, 114:84-97.

Frenzen, P. M., Krasny, M. E., and Rigney, L. P. (1988), Thirty-tree years of plant succession on the Kautz Creek mudflow, Mount Rainier National Park, Washington, *Canadian Journal of Botany* 66:130-137.

Halpern, C. B., and Franklin, J. F. (1990), Physiognomic development of *Pseudotsuga* forests in relation to initial structure and disturbance intensity, *Journal of Vegetation Science* 1:475-482.

Halpern, C. B., Frenzen, P. M., Means, J. E., and Franklin, J. F. (1990), Plant succession in areas of scorched and blown-down forest after the 1980 eruption of Mount St. Helens, Washington, *Journal of Vegetation Science* 1:181-194.

Halpern, C. B., and Harmon, M. E. (1982), Early plant succession on the Muddy River mudflow, Mount St. Helens, Washington, *The American Naturalist* 110:97-106.

Kiilsgaard, C. W., Greene, S. E., Stafford, S. G., and McKee, W. A. (1986), Recovery of riparian vegetation in the northeastern region of Mount St. Helens, In *Mount St. Helens -- Five Years Later* (S. A. C. Keller, Ed.), Eastern Washington University Press, Cheney, WA., p. 222-230.

Lawrence, R. L., and Ripple, W. J. (in press), Comparisons Among Vegetation Indices and Bandwise Regression in a Highly Disturbed, Heterogeneous Landscape: Mount St. Helens, Washington, *Remote Sensing of Environment*.

Lipman. P. W., and Mullineaux, D. R., Eds. (1981), *The Eruptions of Mount St, Helens, Washington*, Geological Survey Professional Paper 1250, U.S. Government Printing Office, Washington, D.C. 844 p.

MathSoft, Inc. (1995), *S-PLUS Users' Manual*, MathSoft, Inc., Seattle.

Means, J. E., McKee, W. A., Moir, W. H., and Franklin, J. F. (1982), Natural revegetation of the northeastern portion of the devastated area, In *Mount St. Helens -- Five Years Later* (S. A. C. Keller, Ed.), Eastern Washington University Press, Cheney, WA, pp. 93-103.

Smathers, G. A., and Mueller-Dombois, D. (1974), *Invasion and Recovery of Vegetation After a Volcanic Eruption in Hawaii*, National Park Service, Scientific monograph series, no. 5.

Ugolini, F. C., Dahlgren, R., LaManna, J., Nuhn, W., and Zachara, J. (1991), Mineralogy and weathering processes in recent and Holocene tephra deposits of the Pacific Northwest, U.S.A., *Geoderma* 51:277-299.

Venables, W. N., and Ripley, B. D. (1994), *Modern Applied Statistics with S-Plus*, Springer, New York.

Vitousek, P. M., and Walker, L. R. (1987), Colonization, succession and resource availability: ecosystem-level interactions, In *Colonization, Succession and Stability* (A. J. Gray, M. J. Crawley, and P. J. Edwards, Eds.), Blackwell Scientific Publications, Oxford.

Voight, B. (1981), Time scale of the first moments of the May 18 eruption, In *The 1980 Eruptions of Mount St. Helens, Washington* Geological Survey Professional Paper 1250 (P. W. Lipman and D. R. Mullineaux, Eds.), U.S. Government Printing Office, Washington, D.C. p. 69-86.

Waitt, R. B., Hansen, V. L., Sarna-Wojcicki, A. M., and wood, S. H. (1981), Proximal air-fall deposits of eruptions between May 24 and August 7, 1980 -- stratigraphy and field sedimentology, In *The 1980 Eruptions of Mount St. Helens, Washington*

Geological Survey Professional Paper 1250 (P. W. Lipman and D. R. Mullineaux, Eds.), U.S. Government Printing Office, Washington, D.C. p. 617-628.

Wood, D. M., and del Moral, R. (1987), Mechanisms of early primary succession in subalpine habitats on Mount St. Helens, *Ecology* 68:780-790.

Zobel, D. B., and Antos, J. A. (1997), A decade of recovery of understory vegetation buries by volcanic tephra from Mount St. Helens, *Ecological Monographs* 67:317-344.

Chapter 5. Conclusions

The 1980 eruption of Mount St. Helens provided extensive opportunities for research for scientists involved in ecosystem responses to natural disturbances. The research reported in this dissertation demonstrated that valuable opportunities exist for remote sensing scientists. In this research, I sought to accomplish three tasks: (1) develop a method for determining vegetation amount across the Mount St. Helens devastated landscape; (2) characterize the patterns of vegetation succession in this landscape during the years from 1980 to 1995; and (3) determine the relative influence of various ecological factors on these patterns of succession.

The Mount St. Helens landscape exhibits substantial heterogeneity both in amount of vegetation cover and in substrate types. This heterogeneity made it difficult to determine the amount of vegetation present using satellite imagery. Therefore, I compared widely used vegetation indices, soil-adjusted vegetation indices, and multiple regression on raw spectral bands. Contrary to expectations, soil-adjusted indices performed worse than non-adjusted indices. This result was explained by the particular soil reflectance properties of the study site. Further, a vegetation index that used middle infrared bands performed substantially worse than indices using only red and near infrared bands. This result was explained by the high variability of soil reflectances in the middle infrared bands.

The best method for predicting vegetation cover for Mount St. Helens came not from using vegetation indices, as is common practice, but from performing multiple regression on raw spectral bands. My final multiple regression model only used the red and near infrared bands, as did the best vegetation indices. However, by using multiple regression on non-indexed spectral bands, I was able to model separately each of these bands. As a result, the final regression model for Mount St. Helens explained 75% of the variation in vegetation cover. This performance was comparable to studies using vegetation indices with higher vegetation cover and less soil influence.

My findings regarding the usefulness of vegetation indices have important implications for future remote sensing studies. Vegetation indices have been the primary means used for 30 years to predict ecological variables from satellite images. However, I have demonstrated that multiple regression against non-indexed spectral bands can perform better and will not perform worse than vegetation indices.

To characterize succession over the study period, I developed a new approach to satellite image change detection. Traditional methods have either concentrated on year-to-year changes or have used methods that concentrate on the statistical variation in multitemporal data without directly relating the variability to ecological patterns. Borrowing concepts applied in plant community ecology and biometrics, I fit growth curves to a set of eight images captured during the study period. These growth curves related directly to changes in vegetation amount during the period. Ecological parameters of interest were then extracted from the curves and returned to a GIS for spatially explicit ecological analysis.

Using growth curves to characterize vegetation change with satellite images has important advantages over traditional approaches. First, this method is the critical first step in linking remote sensing and GIS to biometrics. Characterizing vegetation growth through curves related to the growth properties of vegetation is a necessary element for predicting growth based on biological, rather than purely statistical, responses. Second, for ecological studies, growth curves characterize the biological response of vegetation. Therefore, the parameters extracted from growth curves relate directly to biological responses, rather than being statistical parameters that might, by chance, be correlated to biological responses.

The techniques I developed for determining vegetation amount across the study area and characterizing vegetation change during the study period were necessary precursors to analyzing the processes responsible for these vegetation patterns. The ultimate purpose of my research was to examine ecological processes that had been observed at Mount St. Helens in fine-scale studies and determine their relative importance at landscape scales. The specific findings that I tested related to the importance of biotic legacies, topography, streams, roads, and pre-eruption vegetation conditions. The explanatory variables I examined to test these findings included type of disturbance, topographical variables, distance from seed sources, distance from the crater, distance from streams, distance from roads, tephra thickness, and pre-eruption conditions.

By far the most important factor in recovery was the presence or absence of biotic legacies. Disturbance types that initiated primary succession showed significantly slower recovery than areas of secondary succession. This is fully consistent with previous studies. The conditions of primary succession, including lack of propagules and nitrogen poor soils, lead to slow vegetation growth. Under secondary succession, the absence of competition following disturbance leads to rapid growth. The presence of both types of succession at Mount St. Helens side-by-side enabled me to quantify the difference in recovery rates during the study period.

Within areas where biotic legacies were present, gradients of legacies were particularly important in early succession. With increased time, factors that influenced the relative success of surviving vegetation became increasingly important, including initial tephra thickness and erosional processes.

Where biotic legacies were absent, factors affecting the success of colonizing seeds were significant. Areas close to forested edges had relatively fast recovery rates. Areas farther from forested edges that were dependent on widely dispersing seeds were greatly influenced by conditions that ameliorated site conditions. The most important of these factors was slope gradient. Steeper slopes experienced rill and gully erosion, which provided relatively safe sites for seedling establishment.

Topographic factors other than slope gradient were less important. Generally, elevation was not a major influence on recovery, although elevation influence increased with time after the eruption. This change over time might reflect a change in species composition or dominance. The limited importance of topographic aspect might be a result of disturbance type being correlated with aspect.

Neither streams nor roads were important in our analysis, except for areas that were not vegetated prior to the eruption. I was not able to determine whether this finding was the result of image resolution or lack of landscape-scale importance of these factors.

Similarly, pre-eruption vegetation conditions were not important, except for areas that were not vegetated prior to the eruption. This finding might have been the result of my combining recent clearcut and meadow classes.

As with previous studies at Mount St. Helens, I was not able to explain a substantial portion of the variability in the successional patterns. Part of this unexplained variation was the result of data quality, including image processing and accuracy of GIS layers. However, previous research has noted that a large amount of variability can be attributed to stochastic factors. Wind patterns, climatic variability, and other chance events have a major influence over vegetation recovery, yet cannot be modeled. Nevertheless, this study was able to discern the relative impact of processes that had been observed at fine scales.

There are several logical extensions of this study. First, the methods I have developed are directly applicable to the planted forests within the Mount St. Helens blast zone. Most of the data to conduct such a study are already present. However, applying methods and data to planted forests would permit several advancements in the fields of remote sensing and ecology. First, meaningful response parameters should related to forest productivity, such as biomass, leaf area, or intercepted photosynthetically active radiation. Second, because data on planted species are available, the study could incorporate the impact of species type. Finally, ground data might be linked to ongoing studies using digital analysis of aerial photographs.

Beyond Mount St. Helens, the analytical approach used in Chapter 4 can be readily applied to other landscapes that have experienced large-scale disturbances. One obvious study site is Yellowstone following the 1988 fires. The extensive fine-scale research that has been conducted at Yellowstone can be extended and tested at landscape scales.

The technical developments contained in my research should also be extended. My method of fitting growth curves to multitemporal data should be refined in two ways. First, a method should be developed for automatically fitting growth curves and extracting parameters of interest on a pixel-by-pixel basis. This would enhance the method for landscapes that are less readily stratified by statistical clustering than Mount St. Helens. Second, using non-linear growth functions, rather than polynomial curves, would allow more flexible curve fitting.

Although my findings are important for understanding the recovery of Mount St. Helens following the 1980 eruptions, the value of my research depends as well on its utility for future research. The suggestions listed are only a few of what I hope will be many opportunities that other researchers and I will pursue in the future.

Bibliography

Andersen, D. C., and MacMahon, J. A. (1985), The effects of catastrophic disturbance: the residual mammals at Mount St. Helens, *Journal of Mammalogy* 66:581-589.

Anderson, G. L., Hanson, J. D., and Haas, R. H. (1993), Evaluating Landsat thematic mapper derived vegetation indices for estimating above-ground biomass on semiarid rangelands, *Remote Sensing of Environment* 45:165-175.

Antos, J. A., and Zobel, D. B. (1987), How plants survive burial: a review and initial responses to tephra from Mount St. Helens, In *Mount St. Helens 1980, Botanical consequences of the Explosive Eruptions* (D. E. Bilderback, Ed.), University of California Press, Berkeley. p. 246-261.

Armesto, J. J., and Pickett, S. T. A. (1986), Removal experiments to test mechanisms of plant succession in oldfields, *Vegetatio* 66:85-93.

Baret, F., Guyot, G., and Major, D. (1989), TSAVI: a vegetation index which minimizes soil brightness effects on LAI of APAR estimation, in *13th Canadian Symposium on Remote Sensing and IGARSS'90*, Vancouver, Canada, 10-14 July.

Boyd, D. S., and Ripple, W. J. (1997), Potential vegetation indices for determining global forest cover, *International Journal of Remote Sensing* 18:1395-1401.

Breiman, L., Friedman, J. H., Olshen, R. A., and Stone, C. J. (1984), *Classification and Regression Trees*, Wadsworth International Group, Belmont, CA.

Chen, J. M., and Cihlar, J. (1996), Retrieving leaf area index of boreal conifer forests using Landsat TM images, *Remote Sensing of Environment* 55:153-162.

Cihlar, J., St.-Laurent, L., and Dyer, J. A. (1991), Relation between the normalized difference vegetation index and ecological variables, *Remote Sensing of Environment* 35:279-298.

Collins, J. B., and Woodcock, C. E. (1996), An assessment of several linear change detection techniques for mapping forest mortality using multitemporal Landsat TM Data, *Remote Sensing of Environment* 56:66-77.

Connell, J. H., and Slatyer, R. O. (1977), Mechanisms of succession in natural communities and their role in community stability and organization, *American Naturalist* 111:1119-1144.

Coppin, P. R., and Bauer, M. E. (1996), Digital change detection in forest ecosystems with remote sensing imagery, *Remote Sensing Reviews* 13:207-234.

Crist, E. P., and Cicone, R. C. (1984), Application of the Tasseled Cap concept to simulated Thematic Mapper data, *Photogrammetric Engineering and Remote Sensing* 50:343-352.

del Moral, R. (1983), Initial recovery of subalpine vegetation on Mount St. Helens, Washington, *American Midland Naturalist* 109:72-80.

del Moral, R., and Bliss, L. C. (1993), Mechanisms of primary succession: insights resulting from the eruption of Mount St. Helens, In *Advances in Ecological Research*, vol. 24 (M. Began and A. Fitter, Eds.), Academic Press, London, pp. 1-66.

del Moral, R., and Wood, D. M. (1993), Early primary succession on the volcano Mount St. Helens, *Journal of Vegetation Science* 4:223-234.

Dusek, D. A., Jackson, R. D., and Musick, J. T. (1985), Winter wheat vegetation indices calculated from combinations of seven spectral bands, *Remote Sensing of Environment* 18:255-267.

Eastman, J. R., and Fulk, M. (1993), Long sequence time series evaluation using standardized principal components, *Photogrammetric Engineering and Remote Sensing* 59:1307-1312.

Efron, B., and Tibshirani, R. (1991), Statistical data analysis in the computer age, *Science* 253:390-395.

Egler, F. E. (1954), Vegetation science concepts. I. Initial floristic composition, a factor in old-field vegetation development, *Vegetatio* 4:412-417.

Elvidge, C. D., and Lyon, R. J. P. (1985), Influence of rock-soil spectral variation on assessment of green biomass, *Remote Sensing of Environment* 17:265-279.

ERDAS (1995), *ERDAS Field Guide*, 3rd ed., ERDAS, Inc, Atlanta, GA, 628 p.

Franklin, J. F., Frenzen, P. M., and Swanson, F. J. (1988), Re-creation of ecosystems at Mount St. Helens--contrasts in artificial and natural approaches, In *Rehabilitating Damaged Ecosystems* (J. Cairns, Ed.), CRC Press, Boca Raton, FL., pp. 1-37.

Franklin, J. F., MacMahon, J. A., Swanson, F. J., and Sedell, J. R. (1985), Ecosystem responses to the eruption of Mount St. Helens, *National Geographic Research* 1:198-216.

Frenzen, P. M. (1992), Mount St. Helens -- a laboratory for research and education, *Journal of Forestry* 90:14-18, 37.

Frenzen, P. M., and Franklin, J. F. (1985), Establishment of conifers from seed on tephra deposited by the 1980 eruptions of Mount St. Helens, Washington, *American Midland Naturalist*, 114:84-97.

Frenzen, P. M., Delano, A. M., and Crisafulli, C. M., comps. (1994), *Mount St. Helens: Biological Responses Following the 1980 Eruptions -- An Indexed Bibliography and Research Abstracts (1980-93)*, Gen. Tech. Rep. PNW-GTR-342, Portland, OR: U.S. Department of Agriculture, Forest Service, Pacific Northwest Research Station, 149 p.

Frenzen, P. M., Krasny, M. E., and Rigney, L. P. (1988), Thirty-tree years of plant succession on the Kautz Creek mudflow, Mount Rainier National Park, Washington, *Canadian Journal of Botany* 66:130-137.

Friedl, M. A., Davis, F. W., Michaelsen, J., and Moritz, M. A. (1995), Scaling and uncertainty in the relationship between the NDVI and land surface biophysical variables: an analysis using a scene simulation model and data from FIFE, *Remote Sensing of Environment* 54:233-246.

Halpern, C. B., and Franklin, J. F. (1990), Physiognomic development of *Pseudotsuga* forests in relation to initial structure and disturbance intensity, *Journal of Vegetation Science* 1:475-482.

Halpern, C. B., and Harmon, M. E. (1982), Early plant succession on the Muddy River mudflow, Mount St. Helens, Washington, *The American Naturalist* 110:97-106.

Halpern, C. B., Frenzen, P. M., Means, J. E., and Franklin, J. F. (1990), Plant succession in areas of scorched and blown-down forest after the 1980 eruption of Mount St. Helens, Washington, *Journal of Vegetation Science* 1:181-194.

Heger, L. (1968), A method of constructing site-index curves from stem analyses, *The Forestry Chronicle* 21:11-15.

Hoblitt, R. P., Miller, C. D., and Vallance, J. W. (1981), Origin and stratigraphy of the deposit produced by the May 18 directed blast, In The 1980 Eruptions of Mount St. Helens, Washington (Lipman, P. W., and Mullineaux, D. R., Eds), U.S. Government Printing Office, Washington, D. C., pp. 401-419

Huete, A. R. (1988), A soil-adjusted vegetation index (SAVI), *Remote Sensing of Environment* 29:295-309.

Huete, A. R., and Jackson, R. D. (1988), Soil and atmosphere influences on the spectra of partial canopies, *Remote Sensing of Environment* 25:89-105.

Hunt, R. (1982), *Plant Growth Curves: The Functional Approach to Plant Growth Analysis*, University Park Press, Baltimore. 248 p.

Jordan, C. F. (1969), Derivation of leaf-area index from quality of light on the forest floor, *Ecology*, 50:663-666.

Kauth, R. J., and Thomas, G. S. (1976), The Tasselled Cap – a graphic description of the spectral-temporal development of agricultural crops as seen by Landsat, In *Proceedings of the symposium on Machine Processing of Remotely Sensed Data*, Purdue University, West Lafayette, IN. pp. 51-51.

Kiilsgaard, C. W., Greene, S. E., Stafford, S. G., and McKee, W. A. (1986), Recovery of riparian vegetation in the northeastern region of Mount St. Helens, In *Mount St. Helens -- five years later* (S. A. C. Keller, Ed.), Eastern Washington University Press, Cheney, WA., p. 222-230.

Lambin, E. F., and Strahler, A. H. (1994), Change vector analysis in multitemporal space: a tool to detect and categorize land-cover change processes using high temporal-resolution satellite data, *Remote Sensing of Environment* 48:231-244.

Lawrence, R. L., and Ripple, W. J. (in press), Comparisons Among Vegetation Indices and Bandwise Regression in a Highly Disturbed, Heterogeneous Landscape: Mount St. Helens, Washington, *Remote Sensing of Environment.*

Levin, S. (1992), The problem of pattern and scale in ecology, *Ecology* 73:1943-1967.

Lillesand, T. M., and Kiefer, R. W. (1994), *Remote Sensing and Interpretation*, 3rd ed., John Wiley & Sons, Inc., New York, 750 p.

Lipman. P. W., and Mullineaux, D. R., Eds. (1981), *The Eruptions of Mount St, Helens, Washington*, Geological Survey Professional Paper 1250, U.S. Government Printing Office, Washington, D.C. 844 p.

Markham, B. L., and Barker, J. L. (1986), Landsat MSS and TM post-calibration dynamic ranges, exoatmospheric reflectances and at-satellite temperatures, *Landsat Technical Notes* 1:3-8.

MathSoft, Inc. (1995), *S-PLUS Users' Manual*, MathSoft, Inc., Seattle.

Means, J. E., McKee, W. A., Moir, W. H., and Franklin, J. F. (1982), Natural revegetation of the northeastern portion of the devastated area, In *Mount St. Helens -- Five Years Later* (S. A. C. Keller, Ed.), Eastern Washington University Press, Cheney, WA, pp. 93-103.

Montgomery, D. C. (1991), *Design and Analysis of Experiments*, 3rd ed., New York, John Wiley & Sons, 649 p.

Muchoney, D. M., and Haack, B. N. (1994), Change detection for monitoring forest defoliation, *Photogrammetric Engineering and Remote Sensing* 60:1243-1251.

Myneni, R. B., and Williams, D. L. (1994), On the relationship between FAPAR and NDVI, *Remote Sensing of Environment* 49:200-211.

Olsson, H. (1994), Changes in satellite-measured reflectances caused by thinning cuttings in boreal forests, *Remote Sensing of Environment* 50:221-230.

Perry, C. R., and Lautenschlager, L. F. (1984), Functional equivalence of spectral vegetation indices, *Remote Sensing of Environment* 14:169-182.

Peterson, U. (1992), Seasonal reflectance factor dynamics in boreal forest clear-cut communities, *International Journal of Remote Sensing* 13:753-772.

Peterson, U., and Nilson, T. (1993), Successional reflectance trajectories in northern temperate forests, *International Journal of Remote Sensing* 14:609-613.

Qi, J., Chehbouni, A., Huete, A. R., Kerr, Y. H., and Sorooshian, S. (1994), A modified soil adjusted vegetation index, *Remote Sensing of Environment* 48:119-126.

Reed, B. C., Brown, J. F., VanderZee, D., Loveland, T. R., Merchant, J. W., and Ohlen, D. O. (1994), Measuring phenological variability from satellite imagery, *Journal of Vegetation Science* 5:703-714.

Richards, F. J. (1959), A flexible growth function for empirical use, *Journal of Experimental Botany* 10:290-300.

Ripple, W. J. (1985), Asymptotic reflectance characteristics of grass vegetation, *Photogrammetric Engineering and Remote Sensing* 51:1915-1921.

Ripple, W. J. (1994), Determining coniferous forest cover and forest fragmentation with NOAA-9 Advanced Very High Resolution Radiometer data, *Photogrammetric Engineering & Remote Sensing* 60:533-540.

Rondeaux, G., Steven, M., and Baret, F. (1996), Optimization of soil-adjusted vegetation indices, *Remote Sensing of Environment* 55:95-107.

Rouse, J. W., Haas, R. H., Schell, J. A., Deering, D. W., and Harlan, J. C. (1974), Monitoring the vernal advancement and retrogradation (greenwave effect) of natural vegetation, NASA/GSFC Type III Final Report, Greenbelt, Maryland.

Running, S. W., Peterson, D. L., Spanner, M. A., and Teuber, K. B. (1986), Remote sensing of coniferous forest leaf area, *Ecology*, 67:273-276.

Samson, S. A. (1993) Two indices to characterize temporal patterns in the spectral response of vegetation, *Photogrammetric Engineering and Remote Sensing* 59:511-517.

Smathers, G. A., and Mueller-Dombois, D. (1974), *Invasion and Recovery of Vegetation After a Volcanic Eruption in Hawaii*, National Park Service, Scientific monograph series, no. 5.

Spanner, M. A., Pierce, L. L., Running, S. W., and Peterson, D. L. (1990), The seasonality of AVHRR data of temperate coniferous forests: relationship with leaf area index, *Remote Sensing of Environment*, 33:97-112.

Tucker, C. J. (1979), Red and photographic infrared linear combinations for monitoring vegetation, *Remote Sensing of Environment* 8:127-150.

Turner, M. G. (1989), Landscape ecology: the effect of pattern on process, *Annual Review of Ecology and Systematics* 20:171-197.

Ugolini, F. C., Dahlgren, R., LaManna, J, Nuhn, W., and Zachara, J. (1991), Mineralogy and weathering processes in Recent and Holocene tephra deposits of the Pacific Northwest, USA, *Geoderma*, 51:277-199.

Venables, W. N., and Ripley, B. D. (1994), *Modern Applied Statistics with S-Plus*, Springer, New York.

Vitousek, P. M., and Walker, L. R. (1987), Colonization, succession and resource availability: ecosystem-level interactions, In *Colonization, Succession and Stability* (A. J. Gray, M. J. Crawley, and P. J. Edwards, Eds.), Blackwell Scientific Publications, Oxford.

Voight, B. (1981), Time scale of the first moments of the May 18 eruption, In *The 1980 Eruptions of Mount St. Helens, Washington* Geological Survey Professional Paper 1250 (P. W. Lipman and D. R. Mullineaux, Eds.), U.S. Government Printing Office, Washington, D.C. p. 69-86.

Waitt, R. B., Hansen, V. L., Sarna-Wojcicki, A. M., and wood, S. H. (1991), Proximal air-fall deposits of eruptions between May 24 and August 7, 1980 -- stratigraphy and field sedimentology, In *The 1980 Eruptions of Mount St. Helens, Washington* Geological Survey Professional Paper 1250 (P. W. Lipman and D. R. Mullineaux, Eds.), U.S. Government Printing Office, Washington, D.C. p. 617-628.

Wiegand, C. L., Richardson, A. J., Escobar, D. E., and Gerbermann, A. H. (1991), Vegetation indices in crop assessments, *Remote Sensing of Environment* 35:105-119.

Wood, D. M., and del Moral, R. (1987), Mechanisms of early primary succession in subalpine habitats on Mount St. Helens, *Ecology* 68:780-790.

Yoder, B. J., and Waring, R. H. (1994), The normalized difference vegetation index of small Douglas-fir canopies with varying chlorophyll concentrations, *Remote Sensing of Environment* 49:81-91.

Zobel, D. B., and Antos, J. A. (1997), A decade of recovery of understory vegetation buries by volcanic tephra from Mount St. Helens, *Ecological Monographs* 67:317-344.